AD-A179 394 FABRY-PEROT TYPE OPTICAL INTERFERENCE FILTERS(U) 1/1
ELECTRONICS RESEARCH LAB ADELAIDE (AUSTRALIA)
M A FOLKARD ET AL. AUG 86 ERL-0380-TR

UNCLASSIFIED F/G 20/6 NL

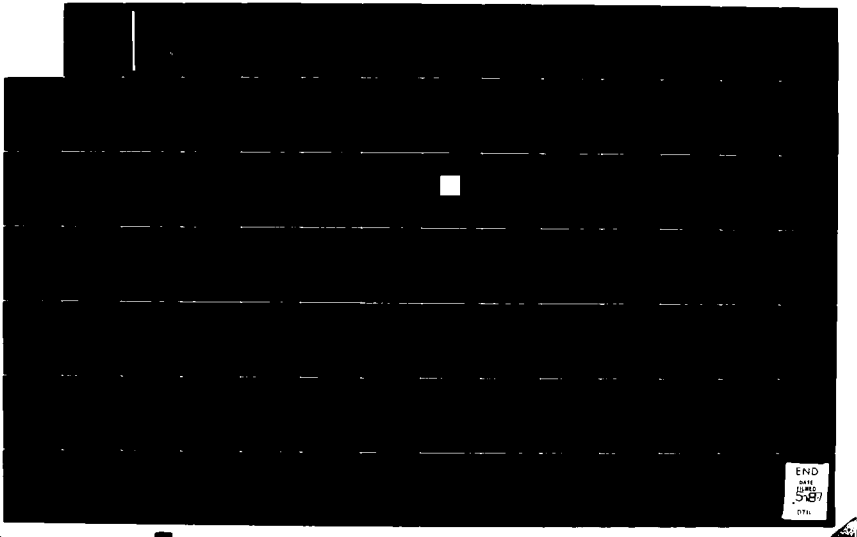

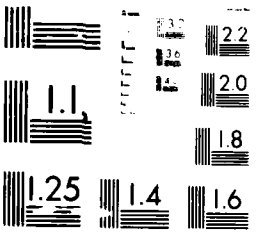

(12)

ERL 0300 TR

AR-003-745

AUSTRALIA

DEPARTMENT OF DEFENCE

DEFENCE SCIENCE AND TECHNOLOGY ORGANISATION

ELECTRONICS RESEARCH LABORATORY

DEFENCE RESEARCH CENTRE SALISBURY
SOUTH AUSTRALIA

TECHNICAL REPORT

ERL-0300-TR

FABRY-PEROT TYPE OPTICAL INTERFERENCE FILTERS

M.A. FOLKARD and J. WARD

Approved for Public Release

AUGUST 1986

COPY No. 43

AR-003-745

DEPARTMENT OF DEFENCE

DEFENCE SCIENCE AND TECHNOLOGY ORGANISATION

ELECTRONICS RESEARCH LABORATORY

TECHNICAL REPORT

ERL-0300-TR

FABRY-PEROT TYPE OPTICAL INTERFERENCE FILTERS

M.A. Folkard and J. Ward

S U M M A R Y

The formulae and theory describing the optical properties of a classical Fabry-Perot interferometer are stated in terms of the reflection, transmission, absorption and phase angle. The appropriate boundary conditions and experimental limitations are defined.

The theory is extended to the production of vacuum deposited, all dielectric, multilayer thin film systems for use as Fabry-Perot type, narrow spectral band filters.

POSTAL ADDRESS: Director, Electronics Research Laboratory,
Box 2151, GPO, Adelaide, South Australia, 5001.

TABLE OF CONTENTS

LIST OF TABLES

LIST OF APPENDICES

LIST OF FIGURES

1. INTRODUCTION

A Fabry-Perot interferometer consists of two semi-reflecting surfaces which are optically flat and parallel to each other and separated by a "Spacer Layer" which can be solid, liquid or gas (figure 1). Light is transmitted through the interferometer in narrow spectral bands the wavelengths of which are determined by the effective optical thickness of the spacer layer.

An optical interference filter is essentially a solid Fabry-Perot interferometer which consists of a series of vacuum deposited layers of dielectric materials followed by a spacer layer which is then followed by another series of dielectric layers (see figure 2). The layers in the reflecting stacks are made from materials having alternately high and low refractive indices. When each layer in the reflecting stack has an optical thickness of one quarter wavelength, the reflections from each successive boundary are in phase and reinforce each other. It is possible to increase the reflectance at the two boundaries of the spacer layer to very high values using these multiple reflections. The central spacer layer acts as a blooming layer, and if correctly made reduces the reflectance of the dielectric reflecting stacks to zero at the wavelength or wavelengths for which the spacer layer is an integral number of half wavelengths in optical thickness, and thereby determines the wavelength at which the filter has its highest transmission. A Fabry-Perot resonator with a fixed spacing is sometimes referred to as an etalon.

The general theory of Fabry-Perot filters is described in Section 2, while Section 3 examines the theory of resonant reflectors. Section 4 concentrates on the theory as it applies to optical interference filters with outer reflectors of multilayer dielectric thin films.

2. FABRY-PEROT ETALONS: SIMPLIFIED THEORY

The theory which describes the reflection and transmission properties of a multilayer interference filter (Fabry-Perot filter), is derived from the reflection, refraction and absorption of light by a thin film(ref.1,2). It is thus appropriate to begin by considering the case of reflection from a thin film with perfectly plane sides which are parallel to each other.

2.1 Reflection from a plane parallel film

With reference to figure 3, let a ray of light from a source S be incident on the surface of such a film at P. This ray is reflected, refracted and transmitted as shown and yields two sets of parallel rays, one on each side of the film. In each of these sets of parallel rays the intensity decreases rapidly from one ray to the next. The optical path difference between the adjacent rays such as rays 1 and 2 is equal to $2nd \cos \theta$

where,

n = refractive index of film

d = physical thickness of film

θ_i = angle of incidence

θ = angle of refraction in the film

Ray 1 is reflected at P from a denser medium back into a less dense medium and suffers a phase change of π relative to rays 2, 3, 4 etc. Destructive interference takes place between rays 1 and 2 and a minimum in reflected intensity is observed when

$$m\lambda = 2nd \cos \theta \qquad (1)$$

where m is an integer known as the "order of interference" or "order number", and λ is the wavelength of the incident light. This condition also describes a maximum in transmitted intensity.

Constructive interference between reflected rays 1 and 2 takes place when

$$\left(m + \frac{1}{2}\right)\lambda = 2nd \cos \theta$$

and this corresponds to a maximum in reflected intensity and a minimum in transmitted intensity.

To derive an equation for the intensity distribution in either the reflected or transmitted interference systems, it is necessary to sum an infinite number of vibrations of diminishing amplitude, paying particular attention to their phase differences. The incident radiation is separated into reflected, transmitted and absorbed components and to avoid confusion, these components are examined in detail in Appendices I, II and III.

2.2 Fabry-Perot Etalons - basic equations

The relationships for the transmitted interference fringes are now considered in terms of the multiple reflections which occur at the various interfaces in a Fabry-Perot interference system. If the film shown in figure 3 represents the spacer layer of an etalon in which every surface is flat and parallel to all the other surfaces, and the two reflecting surfaces bounding the spacer layer are identical, the transmitted intensity I in terms of the incident intensity I_o as derived in Appendix IV is given by

$$I = \frac{I_o T_1^2 e^{-\alpha d}}{(1 - R_1 e^{-\alpha d})^2 + 4 R_1 e^{-\alpha d} \sin^2 \phi} \qquad (2)$$

where T_1 = the single surface transmittance of each of the two identical reflecting surfaces

R_1 = the single surface reflectance of each of the two identical reflecting surfaces which form the boundaries of the central spacer laver

α = the attenuation or absorption coefficient due to absorption within the spacer layer

d = the physical thickness of the spacer layer

ϕ = a frequency dependent phase term consisting of $\phi_S + \phi_R$

where ϕ_R = phase change associated with internal reflection at each boundary of the spacer layer. (This term is examined in detail in Appendix II)

ϕ_S = phase thickness of the spacer layer given by

$$\phi_S = \frac{2\pi}{\lambda} nd \cos\theta$$

The total phase change due to propagation through a layer is therefore given by

$$\phi = \frac{2\pi}{\lambda} nd \cos\theta + \phi_R \qquad (3)$$

In the absence of absorption within the spacer layer ($\alpha = 0$) this expression reduces to the well-known Airy expression(ref.3 and Appendix IV)

$$I = \frac{T_1^2}{(1 - R_1)^2} \cdot \frac{I_0}{1 + F \sin^2 \phi} \qquad (4)$$

where $F = \frac{4R_1}{(1 - R_1)^2}$ is known as the Coefficient of Finesse and $\frac{1}{1 + F \sin^2 \phi}$ is known as the Airy function.

The Airy function represents the transmitted flux density distribution and should not be confused with 'FINESSE', defined in Section 2.7, which is a measure of the resolving power of an etalon.

Note that in equation (4) there is no requirement for zero absorption in the two reflecting mirrors at the surfaces of the spacer layer, only for zero absorption within the spacer layer.

2.2.1 Transmission of incident light of variable wavelength through an etalon of constant optical thickness

When light of variable wavelength is incident upon a filter whose spacer layer is of constant optical thickness, a series of transmission peaks (passbands) will occur at wavelengths λ_m only, where λ_m is determined by the phase term ϕ (see equation (3)).

Maxima in transmission occur when $\sin^2 \phi = 0$, or $\phi = m\pi$, where the integer m is the order number.

The finally transmitted beam intensities of the Fabry-Perot etalon shown in figure 1 consists of a series of interference fringes of equal inclination following the locus of constant angle of incidence upon the top surface. For a plane parallel plate the interference fringes in transmitted light consist of a series of bright narrow rings on a dark background. These are often referred to as Fabry-Perot rings

(figure 4). In the absence of absorption in either the mirrors or the spacer layer, the maximum intensity of the rings is equal to the incident intensity.

The Free Spectral Range of a Fabry-Perot filter is defined as the separation in phase between adjacent orders of interference. In terms of the phase parameter Φ, the free spectral range corresponds to,

$$\Phi_{m+1} - \Phi_m = \pi$$

If for the moment the optical thickness nd' of the spacer layer is considered to include the path equivalent of the phase change Φ_R, ie $nd' = nd \cos \vartheta + \frac{\lambda}{2\pi} \Phi_R$ then the maximum transmission will occur at wavelengths λ_m defined from equation (1) ie $\lambda_m = \frac{2nd'}{m}$.

For a specified effective spacer layer thickness nd', a series of peaks will occur at wavelengths $\frac{2nd'}{1}$, $\frac{2nd'}{2}$, $\frac{2nd'}{3}$, ... $\frac{2nd'}{m}$. These peaks can be displaced to shorter wavelengths by tilting the filter. This happens because the optical path length in the spacer layer decreases with increasing angle of incidence θi according to the relationship $m\lambda_m = 2nd \cos \theta + \frac{\lambda}{\pi} \Phi_R$.

2.2.2 Transmission of incident light of fixed wavelength through an etalon of variable optical thickness

For normal incidence illumination with radiation of wavelength λ, equation (1) shows that the first order of interference will occur when the optical thickness of the spacer layer is $\frac{\lambda}{2}$, the second order when the spacer layer is $\frac{2\lambda}{2}$ and the third is $\frac{3\lambda}{2}$ etc.

2.3 Passband shape and characteristics of an etalon

The general equation derived in Appendix IV and given by Equation (2) allows for any absorption which may be present in both the spacer layer and the mirrors bounding the spacer layer. A more useful form of equation (2) is given by

$$I = \frac{(1 - R_1 - A_1)^2 e^{-\alpha d} I_0}{(1 - R_1 e^{-\alpha d})^2 + 4R_1 e^{-\alpha d} \sin^2 \Phi} \qquad (6)$$

where

$$R_1 + T_1 + A_1 = 1$$

defines the absorptance A_1 of each mirror system in terms of its reflectance R_1 and transmittance T_1. Equation (6) can be simplified for certain cases when there is no absorption present in either the mirrors or the spacer layer.

2.3.1 No absorption in either the mirror system or the spacer layer

When $R_1 + T_1 = 1$ for the mirror system, and $\alpha = 0$ for the spacer layer, then from equation (6),

$$T = \frac{I}{I_0} = \frac{1}{1 + \frac{4R_1}{(1 - R_1)^2} \sin^2 \phi} \tag{7}$$

which is simply the Airy function mentioned in Section 2.2. The "shape" of the transmission curve is determined by the value of R_1 only. Equation (7) is plotted as a function of phase angle ϕ for various values of R_1 in figures 5 and 6. It is seen from these figures that the maximum value for $\frac{I}{I_0}$ of unity occurs when $\phi = 0$ (or $m\pi$) as discussed in Section 2.2.1. It is also clear that the transmission peak becomes increasly narrow as the value of R_1 increases.

2.3.2 Absorption in the mirror system, no absorption in the spacer layer

When $\alpha = 0$ for the spacer layer, equation (6) becomes

$$T = \frac{I}{I_0} = \left(1 - \frac{A_1}{1 - R_1}\right)^2 \cdot \frac{1}{1 + \frac{4R_1}{(1 - R_1)^2} \sin^2 \phi} \tag{8}$$

As in Section 2.3.1, the "shape" of the transmission curve is determined by the Airy function and is quite independent of any absorption which may be present at the reflecting surfaces. However, the magnitude of the maximum transmission now varies with $\left(1 - \frac{A_1}{1 - R_1}\right)^2$.

To demonstrate the effect of absorption in the mirror systems, equation (8) is plotted as a function of phase angle ϕ in figures 7 and 8.

These figures show the effect of changing R_1 for a fixed value $A_1 = 0.01$, and can be compared with figures 5 and 6 respectively, where $A_1 = 0$. Figures 9, 10 and 11 show the effect of changing A_1 where R_1 has fixed values of 0.99, 0.90 and 0.50.

2.3.3 Absorption in the spacer layer, no absorption in the mirror system

When $R_1 + T_1 = 1$ and $\alpha = 0$, equation (6) becomes

$$\frac{I}{I_0} = \frac{e^{-\alpha d}(1 - R_1)^2}{(1 - R_1 e^{-\alpha d})^2 + 4R_1 e^{-\alpha d} \sin^2 \phi} \qquad (9)$$

The maximum transmission is now a function of both thickness and attenuation coefficient, α.

Figure 12 shows the effect of changing R_1 for a fixed value $\alpha d = 0.01$, and can be compared with figures 5 and 7.

Figure 13 shows the effect of changing R_1, when R_1 is close to unity, for a fixed value $\alpha d = 0.01$, and can be compared with figures 6 and 8.

Figures 14, 15 and 16 show the effect of changing αd for fixed mirror reflectivities R_1 of 0.99, 0.90 and 0.5 respectively as the value of αd varies from 0 to 1.0. (Note that $\alpha d = 1.0$ corresponds to an internal intensity transmittance factor of e^{-1}). Figures 14, 15 and 16 can be compared with figures 9, 10 and 11 respectively.

These diagrams clearly demonstrate that high reflectance values are necessary in order to produce narrow bandwidth filters, and that even a small amount of absorption in the mirror system will dramatically reduce the peak transmission levels.

2.3.4 Absorption in both the spacer layer and the mirror system

When absorption is present in both the spacer layer and the mirror system, then the transmitted wave will be attenuated by all parts of the filter, and the full expression of equation (6) will be applicable,

$$T = \frac{I}{I_0} = \frac{e^{-\alpha d}(1 - R_1 - A_1)^2}{(1 - R_1 e^{-\alpha d})^2 + 4R_1 e^{-\alpha d} \sin^2 \phi} \qquad (10)$$

Figures 17 and 18 show the effect of changing the mirror reflectivity R_1 for fixed absorption $A_1 = 0.01$ in the mirror system and $\alpha d = 0.01$ in the spacer layer. Figure 17 should be compared with figures 5, 7 and 12 while figure 18 should be compared with figures 6, 8 and 13.

Figure 19 uses a three dimensional plot to demonstrate the effect on transmission I/I_0 when both A_1 and αd vary with a fixed value of $R_1 = 0.9$.

To assist in comparison within the graphical presentation, the conditions for which each graph is calculated are listed in Table 1.

TABLE 1. SUMMARY OF CONDITIONS USED FOR CALCULATING TRANSMISSION CURVES IN FIGURES 5 TO 19

R_1 varies from 0.1 to 0.9	R_1 varies from 0.90 to 0.99	R_1 = 0.99 fixed	R_1 = 0.90 fixed	R_1 = 0.50 fixed
A_1 = 0 αd = 0 Figure 5	A_1 = 0 αd = 0 Figure 6			
A_1 = 0.01 αd = 0 Figure 7	A_1 = 0.01 αd = 0 Figure 8	A_1 varies from 0 to 0.01 αd = 0 Figure 9	A_1 varies from 0 to 0.10 αd = 0 Figure 10	A_1 varies from 0 to 0.4 αd = 0 Figure 11
A_1 = 0 αd = 0.01 Figure 12	A_1 = 0 αd = 0.01 Figure 13	A_1 = 0 αd varies Figure 14	A_1 = 0 αd varies Figure 15	A_1 = 0 αd varies Figure 16
A_1 = 0.01 αd = 0.01 Figure 17	A_1 = 0.01 αd = 0.01 Figure 18		A_1 varies αd varies Figure 19	

2.4 Definition of contrast

The maximum transmission is obtained by substituting $\phi = 0$ in equation (6). After rearranging, this gives,

$$\frac{I_{max}}{I_0} = \frac{(1 - R_1 - A_1)^2 \, e^{-\alpha d}}{(1 - R_1 e^{-\alpha d})^2}$$

The minimum transmission is obtained by substituting $\phi = \frac{\pi}{2}$, resulting in

$$\frac{I_{min}}{I_0} = \frac{(1 - R_1 - A_1)^2 \, e^{-\alpha d}}{(1 + R_1 e^{-\alpha d})^2}$$

The contrast, defined as the ratio of the maximum to minimum transmission levels is then

$$\text{Contrast} = \frac{I_{max}}{I_{min}} = \frac{1 + R_1 e^{-\alpha d}}{1 - R_1 e^{-\alpha d}} \qquad (11)$$

The contrast is largest when R_1 is large and αd is small, and is independent of A_1.

An alternative form which is sometimes used, defines

$$\text{Contrast} = \frac{I_{max} - I_{min}}{I_{max} + I_{min}} = \frac{2R_1 e^{-\alpha d}}{(1 + R_1^2 e^{-2\alpha d})} \qquad (12)$$

It is evident from these expressions that absorption in the mirrors (A_1) reduces the magnitudes of both maximum and minimum transmission levels, but has no effect on the contrast. However, in some instances, absorption in the spacer layer will markedly reduce the contrast level.

2.5 Definition of half bandwidth (HBW)

The concept of spectral width or half bandwidth (HBW) is often used to characterise the "sharpness" of an interference filter. The half bandwidth of a filter defines the spectral region in which the intensity of the transmitted light is greater than, or equal to, half the maximum transmitted intensity.

For the interference fringe of integral order m, the points where the intensity has dropped to half its maximum value lie at

$$\phi = m\pi \pm 0.5\ \phi_{\frac{1}{2}}$$

where $\phi_{\frac{1}{2}}$ is the half bandwidth in terms of phase angle (figure 20). The half bandwidth $\phi_{\frac{1}{2}}$ can be derived from equation (6) by considering that $I = I_{max}$ when $\phi = 0$ and $I = \frac{I_{max}}{2}$ when $\phi = m\pi \pm 0.5\ \phi_{\frac{1}{2}}$.

ie

$$\frac{1}{2\ (1 - R_1 e^{-\alpha d})^2} = \frac{1}{(1 - R_1 e^{-\alpha d})^2 + 4R_1 e^{-\alpha d} \sin^2 (0.5\ \phi_{\frac{1}{2}})}$$

$$\sin^2 (0.5\ \phi_{\frac{1}{2}}) = \frac{(1 - R_1 e^{-\alpha d})^2}{4R_1 e^{-\alpha d}}$$

$$\sin (0.5\ \phi_{\frac{1}{2}}) = \frac{1 - R_1 e^{-\alpha d}}{2\sqrt{R_1 e^{-\alpha d}}}$$

so

$$\phi_{\frac{1}{2}} = 2 \sin^{-1} \left(\frac{1 - R_1 e^{-\alpha d}}{2\sqrt{R_1 e^{-\alpha d}}} \right)$$

For narrow bandwidth filters, the approximation $\sin (0.5\ \phi_{\frac{1}{2}}) \approx 0.5\ \phi_{\frac{1}{2}}$ can be made, so that half bandwidth in terms of phase is given by

$$\phi_{\frac{1}{2}} \approx \left(\frac{1 - R_1 e^{-\alpha d}}{\sqrt{R_1 e^{-\alpha d}}} \right)$$

In terms of wavelength,

$$\text{HBW} = \frac{\lambda_m}{m\pi} \cdot \phi_{\frac{1}{2}} = \frac{\lambda_m}{m\pi} \left(\frac{1 - R_1 e^{-\alpha d}}{\sqrt{R_1 e^{-\alpha d}}} \right) \ldots \text{reference 8} \qquad (13)$$

where, λ_m = wavelength of peak trasmission of filter, of order 'm'.

It is clear that the HBW of a filter will decrease with:

(i) increasing order m

(ii) increasing reflectivity R_1

(iii) decreasing absorption αd in the spacer layer

For example, a first order filter with a transmission peak at 550 nm has half bandwidths of 3.5 nm, 1.75 nm and 0.175 nm for reflectivities R_1 of 98%, 99%, and 99.9% respectively where there is no absorption in the spacer layer. If the absorption in the spacer layer increases to $\alpha d = 0.01$ then the corresponding HBW's become 5.15 nm, 3.54 nm and 2.64 nm, while if the absorption increases further to $\alpha d = 0.10$ the corresponding HBW's increase to 25.2 nm, 19.3 nm, and 17.5 nm respectively.

The variation of halfbandwidth with changes in mirror reflectance R_1 and spacer absorption αd when $\lambda_m = 550$ nm, is shown in figures 21 and 22.

2.6 Limitations on half bandwidth

The derivations so far have considered a Fabry-Perot etalon with reflecting surfaces perfectly plane and parallel over the entire viewing aperture, and parallel incident illumination normal to the etalon. The HBW is then determined only by the reflectance R_1 and the absorption αd in the spacer layer. In such a situation the spectral bandwidth should become increasingly narrow as $R_1 \to 1$ and $\alpha \to 0$.

2.6.1 Non-plane-parallel layers

However, in practical filter systems the many layers are never completely isotropic, plane and parallel, so that the physical thickness d of the spacer layer always varies over the aperture of the filter. As $R_1 \to 1$ the resultant HBW depends on the form and magnitude of the departure from plane parallelism.

If the surfaces bounding the spacer layer are flat and parallel to within $\frac{\lambda}{f}$ (ie the optical thickness nd changes by $\frac{\lambda}{f}$ between the centre and the edges of the filter aperture, with either a parabolic or linear form of non-uniformity(ref.4)) then the contribution to $\phi_{\frac{1}{2}}$ due to f is given by

$$(\phi_{\frac{1}{2}})_f = \frac{2\pi}{f}$$

so that

$$(HWB)_f = \frac{\lambda_m}{m\pi} (\phi_{\frac{1}{2}})_f = \frac{2\lambda_m}{mf}$$

In more general terms, if Δd is the RMS deviation in thickness due to surface roughness and/or the lack of parallelism of the two reflecting surfaces within the apertures being used, then the contribution to the HBW of $(HBW)_f$ due to this non-flatness can be defined as

$$(HBW)_f = \frac{2n\,\Delta d}{m} \qquad (14)$$

For example, if the surfaces of a first order filter are flat and parallel to within 0.5 nm of optical thickness, then the contribution to HBW caused by this non-parallelism/flatness would be

$$(HBW)_f = 1.0 \text{ nm}$$

For filters with high reflectance, it is evident that the limiting HBW is determined by lack of parallelism of the reflecting surfaces together with scattering and anisotropy within the layers.

There are, in addition, further contributions to the degradation of the HBW which are caused by the measurement conditions. These are:

2.6.2 Diffraction effects

Due to a finite illumination source with an aperture D there is a diffraction effect which produces a contribution for on-axis illumination of(ref.5),

$$(\phi_{\frac{1}{2}})_D = \frac{\pi\, nd}{D^2}$$

or

$$(HBW)_D = \frac{\lambda_m}{m} \cdot \frac{nd}{D^2} = \frac{2\lambda_m^{\,2}}{D^2} \qquad (15)$$

2.6.3 Non-normal illumination

When the filter is used at angles of incidence other than normal then the cone angle γ of the incident radiation causes a shift of the passband in the shorter wavelength direction, a broadening of the passband and a reduction in the peak transmission. The broadening of the passband is given by(ref.6)

$$(HBW)_\gamma = \frac{\lambda_m}{2} \sin^2 \gamma \qquad (16)$$

When the filter is tilted in a conical beam, further spreading and lowering of the passband occurs although the peak transmission is shifted less than in parallel light for the same angle of tilt. Filters with narrow passbands suffer more degeneration of the passband than broader filters. The intensity distribution across the cone has a noticeable effect on the performance of narrow passband filters. A Gaussian intensity distribution has been found to produce less degeneration of the passband than a linear distribution.

2.6.4 Instrumental measuring techniques

The resolution of the instrument on which the filters were measured introduces a contribution $(HBW)_S$.

2.6.5 Total measured half-bandwidth

It is appropriate to express the total measured half bandwidth of the filter as,

$$(HBW)^2 = (HBW)_R^2 + (HBW)_D^2 + (HBW)_f^2 + (HBW)_\gamma^2 + (HBW)_S^2 \qquad (17)$$

where $(HBW)_R$ has been defined in equation (13) as

$$(HBW)_R = \frac{\lambda_m}{m\pi} \cdot \frac{1 - R_1 e^{-\alpha d}}{\sqrt{R_1 e^{-\alpha d}}}$$

2.7 Definition of finesse

The ratio of the separation of adjacent maxima to the half bandwidth of each maximum is known as the "finesse". Thus a filter with narrow HBW will have a high finesse.

Since the separation of adjacent peaks corresponds to a change in phase angle of π, the finesse N is then,

$$N = \frac{\pi}{\phi_{\frac{1}{2}}} = \frac{\lambda_m}{m} \cdot \frac{1}{HBW}$$

So that, in terms of finesse,

$$HBW = \frac{\lambda_m}{m} \cdot \frac{1}{N} \qquad (18)$$

We see from the foregoing expressions that the finesse is greater when the transmission maxima are sharper.

3. RESONANT REFLECTOR

For completeness, it is appropriate to note that multiple Fabry-Perot etalons used in series with each other enable high values of reflectance to be obtained even without the use of optical coatings. Such a device used in place of the output mirror in a laser cavity is often referred to as a resonant reflector(ref.7).

When multiple etalons are used in series with each other, then the resonant peaks produced are much sharper and further apart from each other. The amplitude of the peak reflectance is given by

$$R_{max} = \frac{4r}{(1 + r)^2}$$

where r is the reflectance of each single surface.

If an uncoated etalon is used, the reflectance, r, is given by,

$$r = \left(\frac{n - 1}{n + 1}\right)^2$$

and the maximum reflectance of a multi element reflector is given by

$$R_{max} = \left(\frac{n^N - 1}{n^N + 1}\right)^2 \qquad (19)$$

where n is the refractive index of the plates and N is the number of reflecting surfaces. Using the simple theory outlined above, it is possible to predict the main characteristics of the transmission-reflection curve versus wavelength for a multi-element etalon. The effect of changes in material, plate thickness, coatings etc can be rapidly evaluated with reference to the system reflectance.

As an example, consider a three-plate etalon or resonant reflector which consists of three optically flat quartz plates with a defined thickness separated by two air spacer layers (see figure 23(a)). Also shown (figure 23(b)) is a curve of the reflectance calculated as a function of wavelength for this three plate system whose plates are 2.5 mm thick and separated from each other by a 2.5 mm air gap. Six different resonance effects can occur in such a device.

(i) Within Plate 1 between its front and back surfaces.

(ii) Between Plate 1 and the first surface of Plate 2 through the air gap.

(iii) Within the first air gap.

(iv) Between Plates 1 and 2 including the air gap.

(v) Between Plates 1 and 3 including the air gap between Plates 2 and 3.

(vi) Between Plates 1, 2 and 3 including both air gaps.

As can be seen from figure 23(b) this resonant reflector has a peak reflectance of 65% and the main reflection peak has a half bandwidth of 0.0038 nm. The envelope of the individual resonance peaks is repeated every 0.067 nm.

It should be noted that the resonance within a single plate determines the period of the whole device. The main peaks are caused by the resonance within the air space and the minor peaks are caused by resonances occuring between surfaces which include both air spaces and at least two of the plates.

High resolution resonant reflectors of this type enable extremely narrow spectral regions to be isolated. The analysis of spectral lines, shapes and bandwidths can be more readily determined for a large range of applications.

4. VACUUM-DEPOSITED MULTILAYER FABRY-PEROT INTERFERENCE FILTERS

As described in Section 1 an optical interference filter is essentially a solid Fabry-Perot interferometer consisting of a series of vacuum deposited layers of dielectric materials of alternately high and low refractive index followed by a spacer layer which is then followed by another series of dielectric layers (see figure 2). The apparatus which is used to produce multilayer filters by electron beam deposition under vacuum conditions is described in reference 8. The production of narrow passband filters accurately located with respect to wavelength imposes high tolerances on the thicknesses of the individual layers.

4.1 Notation for multilayer construction

For clarity and convenience, an abbreviated method for describing multilayer constructions is generally used(ref.9) eg HLHLH or B/HLHLH/S defines a series of layers of alternately high and low refractive index, where

H = layer of optical thickness $\frac{\lambda_o}{4}$, constructed of material of high refractive index n_H

L = layer of optical thickness $\frac{\lambda_o}{4}$, constructed of material of low refractive index n_L

λ_o = control wavelength

S = substrate of refractive index n_S

B = medium adjacent to the last layer (often, air)

This notation can readily be extended to include multilayer optical filters eg B/HLH-2L-HLH/S, or B/3-2L-3/S, or most simply, 3-2L-3 describes a filter having the construction shown in figure 2.

With the aid of computers, very complex multilayer thin film calculations can readily be carried out using the method of characteristic matrices(ref.8,9,10). This technique takes into account the many reflections from the various interfaces within a given system.

4.2 High reflectance dielectric multilayer systems

When each layer in the multilayer stack has an optical thickness of one quarter wavelength, the "effective refractive index" of the multilayer system is given by

$$\text{Effective index} = \sqrt{\frac{n_H^{p+1}}{n_L^{p-1}}}$$

where p is the number of layers. This is a well-known and useful concept for effectively replacing a set of multilayers with a single hypothetical layer whose reflection and transmission properties are equivalent to those of the multilayer.

4.2.1 No absorption in the reflecting stacks

For a non-absorbing multilayer stack, the reflections from each successive film boundary are in phase and reinforce each other. It is thus possible to increase the reflectance to very high values using these multiple reflections.

The calculated reflectance for 'p' layers, each with an optical thickness of one quarter wavelength $\frac{\lambda_o}{4}$, and alternatively of high (n_H) and low (n_L) refractive index, is given by reference 9. The layer system must contain an odd number of layers and begin and end with a layer having a high refractive index.

$$R_1 = \left[\frac{n_H^{p+1} - n_L^{p-1} \cdot n}{n_H^{p+1} + n_L^{p-1} \cdot n}\right]^2$$

Typical, calculated reflectances at normal incidence are shown in Table 1 and figure 24 for the following multilayers (zinc sulphide and cryolite) deposited onto glass substrates. The reflectance of a multilayer stack in air increases as the number of layers is increased, and is maximum when the stack is terminated with a high index layer. For the purpose of this calculation, $n_H = 2.3$, $n_L = 1.35$ and $n_S = 1.52$.

TABLE 2. REFLECTANCE OF MULTILAYER STACKS

System	Number of layers	Calculated reflectivity
SHB	1	0.306
SHL ≡ (HL)B	2	0.347
SHLH ≡ (HL)HB	3	0.672
SHLHL ≡ $(HL)^2B$	4	0.731
$(HL)^2HB$	5	0.872
$(HL)^3B$	6	0.898
$S(HL)^3HB$	7	0.954
$S(HL)^4B$	8	0.963
$S(HL)^4HB$	9	0.984
$S(HL)^5B$	10	0.987
$S(HL)^5HB$	11	0.994
$S(HL)^6B$	12	0.996
$S(HL)^6HB$	13	0.998

It is important to realise that the reflectance of a multilayer dielectric film is high only in a limited wavelength region centred about the wavelength λ_o for which the layers have an optical thickness $\frac{\lambda_o}{4}$.

Although the maximum reflectance increases with increasing number of layers, the spectral region having high reflectance will be reduced, as shown in figure 25, which shows the dependence of reflectance on wavelength λ for 5, 7, 9 and 11 alternate films of zinc sulphide and cryolite, each film being $\frac{\lambda_o}{4}$ thick at a wavelength λ_o = 550 nm.

4.2.2 Absorption in the reflecting stacks

In practice, absorption in the layers limits the maximum attainable reflectance to a value less than unity. Reference 11 has shown that the absorption A in a maximally reflecting quarter wave stack is

$$A = \frac{2\tau\, n_o}{n_H^2 - n_L^2} \left[k_H + k_L\right]. \qquad (20)$$

In this equation n_o is the index of the incident medium, n_H and k_H are the optical constants (refractive index and absorption index respectively) of the high index layers and n_L and k_L are the optical constants of the low index layers. This equation is derived for a quarter wave stack composed of an infinite number of layers, but, in practice it holds well for stacks with a reflectance greater than 0.95.

Equation (20) can be expanded to yield

$$A = \frac{2\pi n_o}{n^2_H} [k_H + k_L] \sum_{j=0}^{\infty} \frac{n_L}{n_H}^{2j} \qquad (21)$$

Each term in the foregoing equation corresponds to the absorption in a particular layer of the stack, ie $\frac{2\pi n_o k_H}{n^2_H}$ is the power absorbed in the high index layer adjacent to the the incident medium. Because $n_H > n_L$, equation (21) predicts that each successive layer in the quarter wave stack contributes a decreasing proportion to the total absorption loss of the mirror. This is attributed to the fact that the electric field strength in a dielectric mirror decreases as the substrate is approached. Since each interface in the stack reflects a portion of the incident flux, each successive layer in the stack receives less flux than the layer above it. Consequently, layers immersed deeply within the stack cannot contribute significantly to the total amount of flux absorbed.

Figure 26 depicts the total absorption in reflecting stacks with different numbers of layers having the real refractive indices n_H and n_L of zinc sulphide and cryolite, but with arbitrary absorption indices k_H and k_L in each layer. Values $k_H = k_L = 0.002$ and $k_H = k_L = 0.005$ were chosen for these calculations, and total absorption was deduced from the relationship $R + T + A = 1$. It is apparent that the majority of the total absorption occurs in the four layers adjacent to the incident medium. The reason for selecting materials of high purity and very low absorption coefficients is apparent.

No attempt will be made here to investigate the effect of minimising the absorption of the multilayer reflecting stack used for Fabry-Perot reflectors, other than to state that minimising the absorption is equivalent to maximising R+T, since absorptance A = 1 - (R+T). This observation led reference 11 to consider the design of stacks having lower absorption than a quarter wave stack. Basically, the design procedure consists of decreasing the amount of high index material in the stack by decreasing the thickness of the outermost high index layers. Using this technique, the total absorption can be decreased by approximately 50% over that attainable with a quarter wave stack. It should be noted that this approach is effective only if there is significant difference between the absorption coefficients of the high and low index layers.

4.3 Design considerations for all-dielectric Fabry-Perot interference filters

The major characteristics of an optical interference filter (half bandwidth, transmission, absorption, wavelength location) are determined by many separate factors, some of which are discussed below.

4.3.1 *Effect of spacer layer thickness*

If the optical thickness of the spacer layer is an integral number of half wavelengths $m.\frac{\lambda_o}{2}$, the filter will have a transmission band of order

m centred at wavelength λ_o. Other transmission bands in addition to those determined by $m\lambda_m = 2nd$ are produced because of the wavelength dependence of the reflecting properties of dielectric films (figure 27). These unwanted sidebands can be suppressed by a variety of well-known methods(ref.8).

Figure 28 shows the decrease in HBW which occurs as the optical thickness of the spacer layer is increased, for filters with 11-mL-11 type construction. The HBW for filters centred at 550 nm decreases from 0.23 nm for an 11-2L-11 filter, to 0.16 nm for an 11-4L-11 filter, and to 0.10 nm for an 11-8L-11 filter. It should be noted, that when the spacer layer has a thickness equal to 0.75, 1.0 or 1.25 quarter wavelengths etc, then there will be no Fabry-Perot passband, simply a broad reflecting band.

4.3.2 Layer thickness tolerances

Filters are usually required to transmit at a specified wavelength. Since the optical thickness of the spacer layer must be accurately controlled because $2nd = m\lambda_m$ at the transmission peak λ_m, then a change $\Delta(nd)$ in nd corresponds to a displacement $\delta\lambda_m$ of the transmission band of order m given by

$$\delta\lambda_m = \lambda_m \cdot \frac{\Delta(nd)}{nd}$$

Thus with λ_m = 550 nm, an error of 0.1% in the optical thickness of the spacer results in an error of 0.5 nm in the position of the passband. For filters whose passband is of this order, variations of 0.1% in the thickness of the spacer will be intolerable. The requirement on thickness tolerances is thus very exacting. Figure 29 shows the effect of errors in the thickness of the spacer layer only, assuming that the reflecting stacks introduce no additional error in the wavelength location. Furthermore, thickness errors in the last layer or the last few layers which act as blooming layers of a reflecting stack result in imperfect blooming with a consequent lowering of efficiency and transmission. It should be noted that the ideal Fabry-Perot etalon is asymmetric and will usually require blooming in order to maximise the transmittance.

Because of the physical structure of thermally evaporated layers, there will always be some degree of inhomogeneity across the aperture of an all-dielectric filter. In additional, there may be some loss in transmitted intensity caused by scattering. However, in practice these non-uniformities can be made very small, and all-dielectric filters having half-bandwidths of 0.5 nm can be made routinely. Filters with narrower bandwidths can be made when particular attention is paid to the evaporation conditions(ref.13).

4.3.3 Effect of reflectance

Figure 30 shows the transmission versus wavelength characteristics near the wavelength of peak transmission for filter constructions 9-4L-9 and 11-4L-11 on glass. The glass is coated on one side only. The other side could be bloomed if required in order to maximise the transmission. See figure 30(c). It can be seen that the increased reflectance of the

11 layer reflecting stack produces a narrower passband (0.22 nm) than the 9 layer reflecting stack (0.7 nm). These curves were computed for a control wavelength λ_o of 550 nm. The general trend of decreasing half bandwidth with increasing reflectance is shown in figure 31 for a wide variety of filter constructions.

Increasing the number of layers in the reflecting stacks produces a steady decrease in bandwidth because of the increased reflectance. However, the eventual lack of homgeneity in the spacer layer and the reflecting stacks over the aperture of the filter causes a variation in the wavelength of the transmission band which is greater than the filter bandwidth. This variation may be several tenths of a nanometer, which must then represent the practical lower limit of bandwidth attainable with filters employing evaporated layers(ref.14).

4.3.4 Effect of absorption in the spacer layer only

The filters discussed thus far in Section 4.3 have had no absorption in either the reflecting stacks or the spacer layers, since both zinc sulphide and cryolite are fully transparent in the visible region over which the calculations have been performed.

The use of dielectric materials having some absorption will degrade the performance of narrowband interference filters. In Section 4.2.2 we discussed the effect of absorption on the reflecting stacks, and found that the reflectance was greatly reduced for even small absorption indices k_H and k_L.

If, however, reflecting stacks made from non-absorbing materials are placed on both sides of a hypothetical spacer layer which has some absorption, then passbands such as those displayed in figure 32 are obtained. The spacer layer, denoted by subscript "S" to differentiate it from the "H" and "L" materials in the reflecting stacks, was given the real refractive index n_S appropriate to cryolite, whilst arbitrary values for the absorption index k_S were used. It is evident from figure 32 that only very low values for k_S can be tolerated in the spacer layer before the peak transmission of the filter is reduced to an unacceptable level.

4.3.5 Effect of absorption in all the multilayers

Absorption in any layer of the filter will degrade its optical performance and the more absorbing layers there are in a filter, or the higher the absorption in a given layer, then the greater the effects on half bandwidth and peak transmission.

Reference 10 has considered a filter having (2p + 1) layers with p, $\frac{\lambda}{4}$ thick layers in each reflecting stack, and a first order (m = 1) high refractive index spacer where the spacer layer $\frac{\lambda}{2}$ thick is constructed of the same high refractive index material as that used in the reflecting stacks ($n_S = n_H$, $k_S = k_H$). Its maximum transmittance T_{max} is given in terms of the filter's transmittance in the absence of absorption, T_o, by the following equation

$$T_{max} = T_o[1 + ck_H + dk_L]^{-2}$$

c and d are constants given by

$$c = d = 1 - \frac{n_L^{2\nu-1}}{n_H^{2\nu}} \cdot \frac{\pi n_o}{(n_o n_S + n_H n_L)\ (n_L/n_H)^p}$$

The halfwidth $(HBW)^1$ of the absorbing filter is

$$(HBW)^1 = (HBW)\ (1 + ck_H + dk_L)$$

where (HBW) is the bandwidth of the in the absence of absorption.

Table 3 illustrates the magnitudes of these effects for various narrow band filter designs. The optical constants used in generating Table 3 are $n_H = 2.3$, $n_L = 1.35$, $n_o = 1.00$ and $n_S = 1.52$. It is interesting to note that a small amount of absorption ($k = 0.0002$) in each of the 25 layers in the filter has such a marked effect.

TABLE 3. EFFECT OF ABSORPTION ON TRANSMISSION OF MULTILAYER FILTERS

Filter construction	Number of layers (2p+1)	$\frac{HBW}{\lambda_o}$	$\frac{HBW^1}{\lambda_o}$	$\frac{HBW^1}{HBW}$	T_o	T_{max}	T_{max}/T_o
4-2l- 4	9	0.0342	0.0344	1.006	95.74	94.53	0.987
6-2L- 6	13	0.0118	0.0120	1.017	95.74	92.27	0.964
8-2L- 8	17	0.0042	0.0043	1.024	95.74	86.18	0.900
10-2L-10	21	0.00140	0.00162	1.157	95.74	71.55	0.747
12-2L-12	25	0.00048	0.00070	1.458	95.74	45.23	0.472
14-2L-14	29	0.00018	0.00038	2.111	95.74	17.78	0.186
16-2L-16	33	0.00006	0.00028	4.667	95.74	4.10	0.043

Figure 33 shows the effect of different absorption coefficients on the passband shape and transmission characteristics of an 11-4L-11 filter. For purposes of this calculation, the chosen absorption coefficient is constant for all the layers in the 11-4L-11 filter.

Finally, with respect to absorption in Fabry-Perot type multilayers, it should be noted that the spatial or total absorption can be tailored to suit a particular requirement, and multilayer systems with their absorption maximised for example in either the Spacer Layer, outermost layers (adjacent to the incident medium) or a combination of both might result in the development of new temperature sensitive Fabry-Perot filters with properties which would vary with temperature(ref.15).

Current methods for computing multilayer characteristics calculate R and T separately, and derive A from the relationship R + T + A = 1. When considering the above proposal for a thermally sensitised Fabry-Perot filter, caution should be exercised in computing for it is necessary to introduce the absorption into a given layer or layers prior to deriving R and T.

4.3.6 *Effect of angle of incidence on passband*

As mentioned in Section 2, the effect of increasing the angle of incidence is to shift the passband peak wavelength location towards the shorter wavelength region. For small angles of tilt (up to say 16°) there are only minor polarisation effects and the width and peak transmission of the passband remain approximately constant. These trends are shown in figure 34 which gives the passband shape and location for an 11-4L-11 filter at angles of incidence up to 60° in parallel light.

It is apparent from figure 35 that the shift in the wavelength of peak transmission does not vary linearly with the angle of tilt. If we express the shift $(\lambda_o - \lambda)$ in terms of λ_o, the wavelength of peak transmission at normal incidence, then,

$$\frac{(\lambda_o - \lambda)}{\lambda_o} \text{ is proportional to } \theta_i^2$$

where θ_i is the angle of incidence in degrees (see for instance reference 15). Figure 36 shows a graph of these quantities taken from the computed performance curve for an 11-4L-11 filter.

5. CONCLUSION

This report is not intended to be an all embracing detailed theoretical and experimental survey of all matters pertaining to Fabry-Perot filter systems. The authors have culled the information for this monograph from a wide range of sources and brought together for the first time, to their knowledge, sets of basic equations describing the optical properties of Fabry-Perot filter systems.

6. ACKNOWLEDGEMENT

The authors gratefully acknowledge the many useful discussions about Fabry-Perot filters held with John Venning and fully appreciate his many suggestions. Much of the computing was ably carried out by Peter Girdler and we thank him for his hours at the console.

REFERENCES

No.	Author	Title
1	Born, M. and Wolf, E.	"Principles of Optics". Pergamon Press, p.358, 1959
2	Jenkins, F.A. and White, H.E.	"Fundamentals of Physical Optics". p.83, 1937
3	Airy, G.B.	Phil. Mag. Vol.2 p.20 (1833)
4	Ramsay, J.V.	"Aberrations of Fabry-Perot Interferometers When Used as Filters". Applied Optics, Vol.8, No.3, p.569-574, March 1969
5	Perkin-Elmer	"Determining the Thickness of a Sealed Cell and Polymer Film by the Interference Fringe Technique". Handbook of Infra-red Spectroscopy, 9/74
6	Brown, M.S.	"The Influence of Tilt, Cone Angle and Beam Intensity Cross Section on the Computed Performance of Narrow Band, Optical Interference Filters". WRE Technical Note 710 (AP), July 1972
7	Koechner, W.	"Solid-State Laser Engineering". Springer-Verlag, New York, Heidelberg Berlin, Fabry-Perot Resonators, p.204, 1976
8	Ward, J.	"Designing and Making Thin Films for Use as Optical Filters". WRE Technical Memorandum ISD90, March 1965
9	Vasicek, A.	"Optics of Thin Films". North Holland Publishing Company, Amsterdam, p.56, 1960
10	Brown, M.S.	"Thin Film Filters Designed by the Method of Equivalent Layers". WRE Technical Note 903 (AP), March 1973
11	Koppelmann, G.	"The Theory of Multilayers Consisting of Weakly Absorbing Materials and Their Use as Interferometer Mirrors". Ann. Phys. (Leipzig), Folg 7, Vol.5, No.7-8, 388-96, 1960
12	MacDonald, J.	"Metal Dielectric Multilayers". Adam Hilger, London, 1971
13	Ward, J. and Paterson, R.	"Thickness Control System for Multilayer Optical Thin Film Work". Australian Patent Number 406, 591, 5 May 1969

No.	Author	Title
14	Netterfield, R.P., Schaeffer, R.C. and Sainty, W.G.	"Coating Fabry-Perot Interferometer Plates with Broadband Dielectric Mirrors". Applied Optics, Vol19, No.17, p.3010, 1 September 1980
15	Folkard, M.A. and Ward, J.	"Exploration of a Concept for Converting an Infrared Image Into a Visible Image". Technical Report ERL 0303 DRCS, July 1986

THIS IS A BLANK PAGE

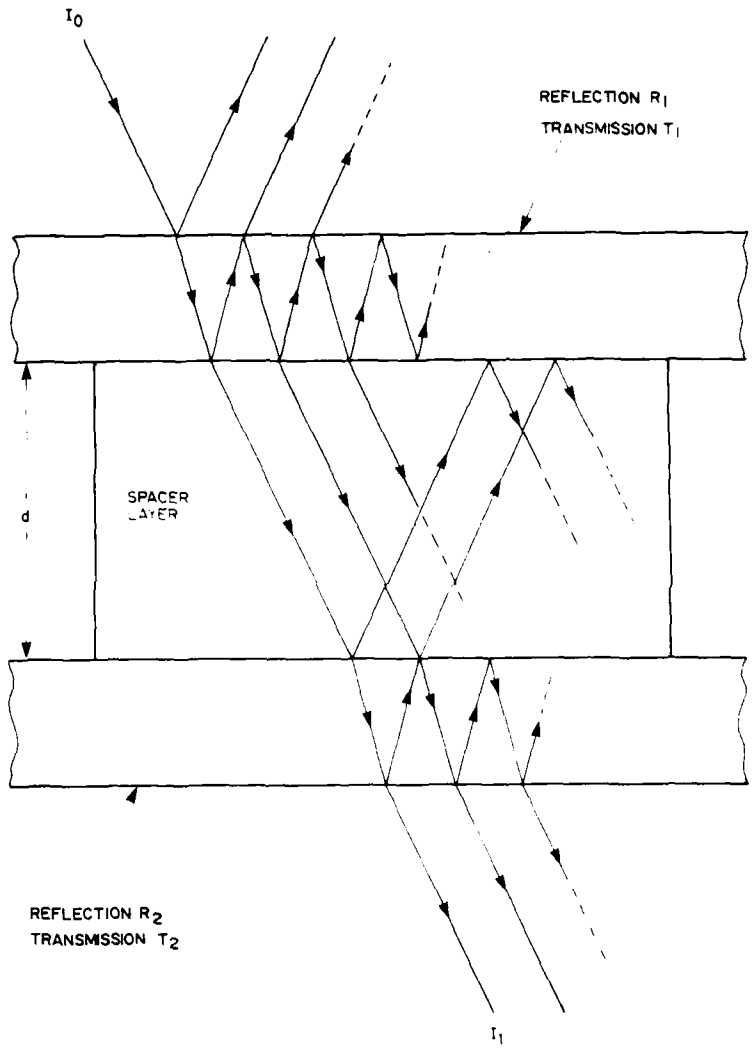

Figure 1. Schematic diagram of a Fabry-Perot interferometer

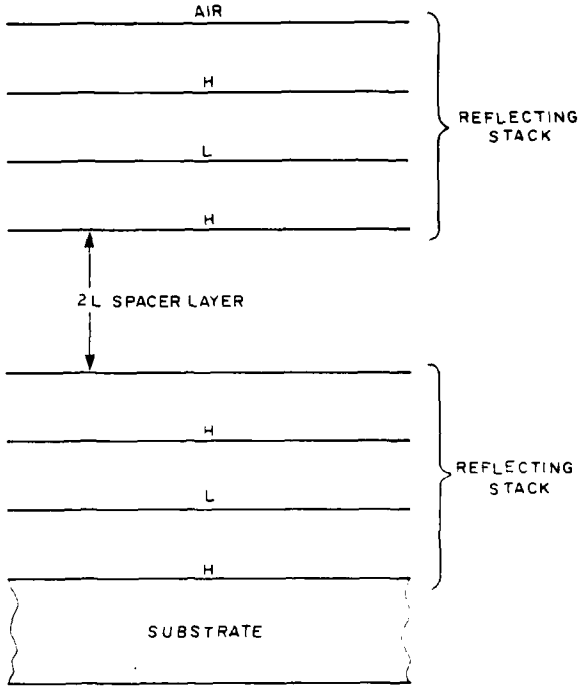

H = quarter wavelength thick layer of material with high refractive index

L = quarter wavelength thick layer of material with low refractive index

Figure 2. An example of a Fabry-Perot Optical Interference Filter

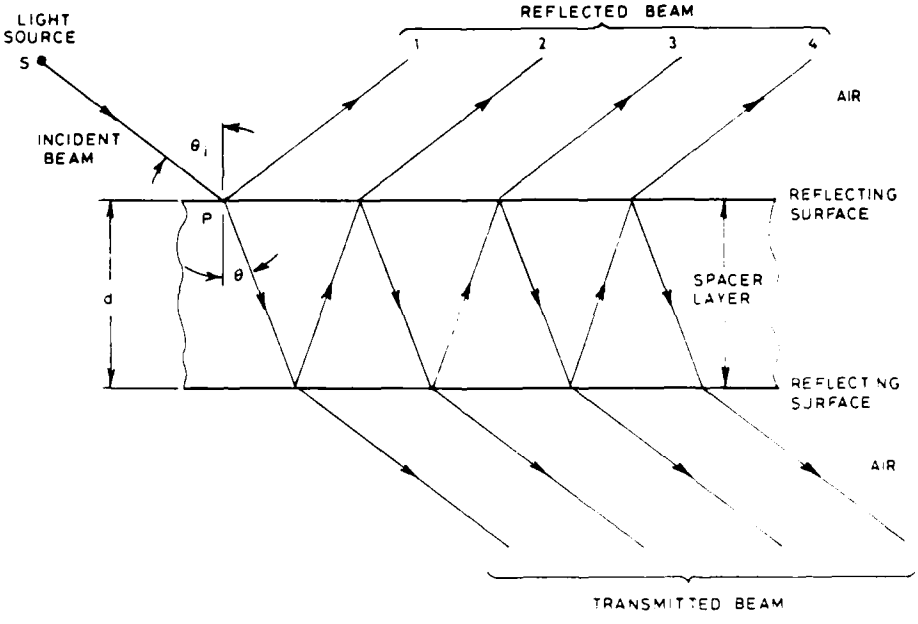

Figure 3. Reflection from a plane parallel film

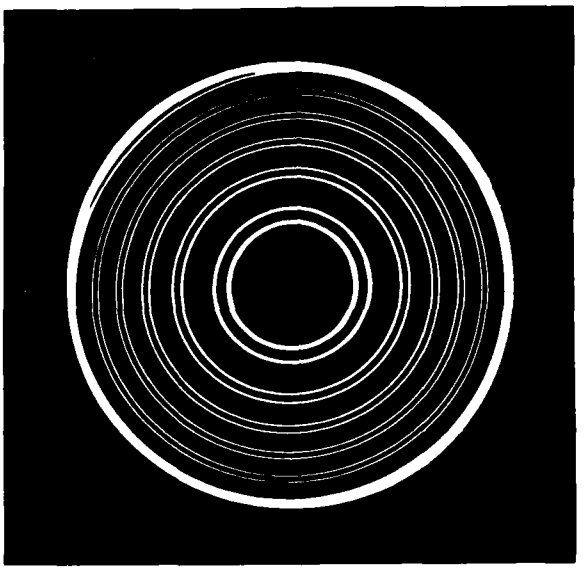

150 mm DIAMETER FABRY-PEROT PLATE

Sodium D lines are shown in pairs above. Slightly out of focus due to shaking of concrete block. Exposure 30 s on 300 ASA film

Figure 4. Fabry-Perot rings

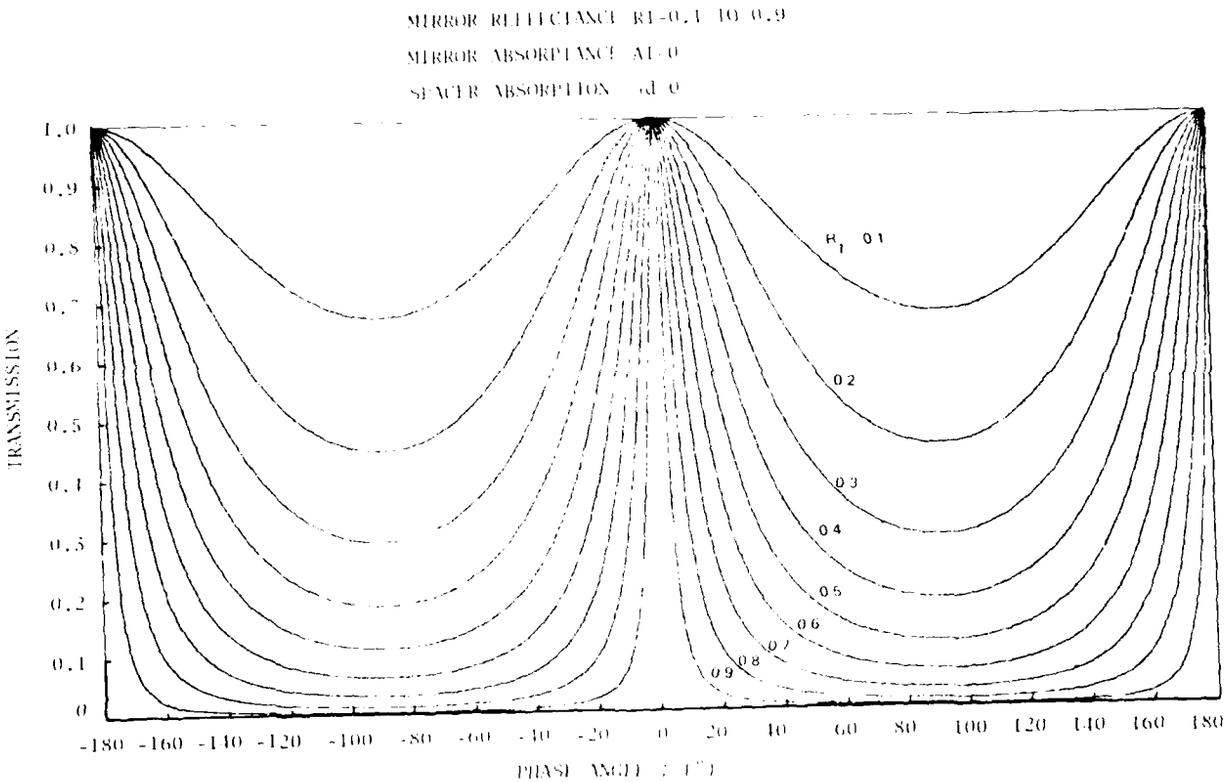

Figure 5. Effect on transmission of variable reflectance R_1, when there is no absorption in either the spacer layer or the mirrors ($R_2 = 0.9$)

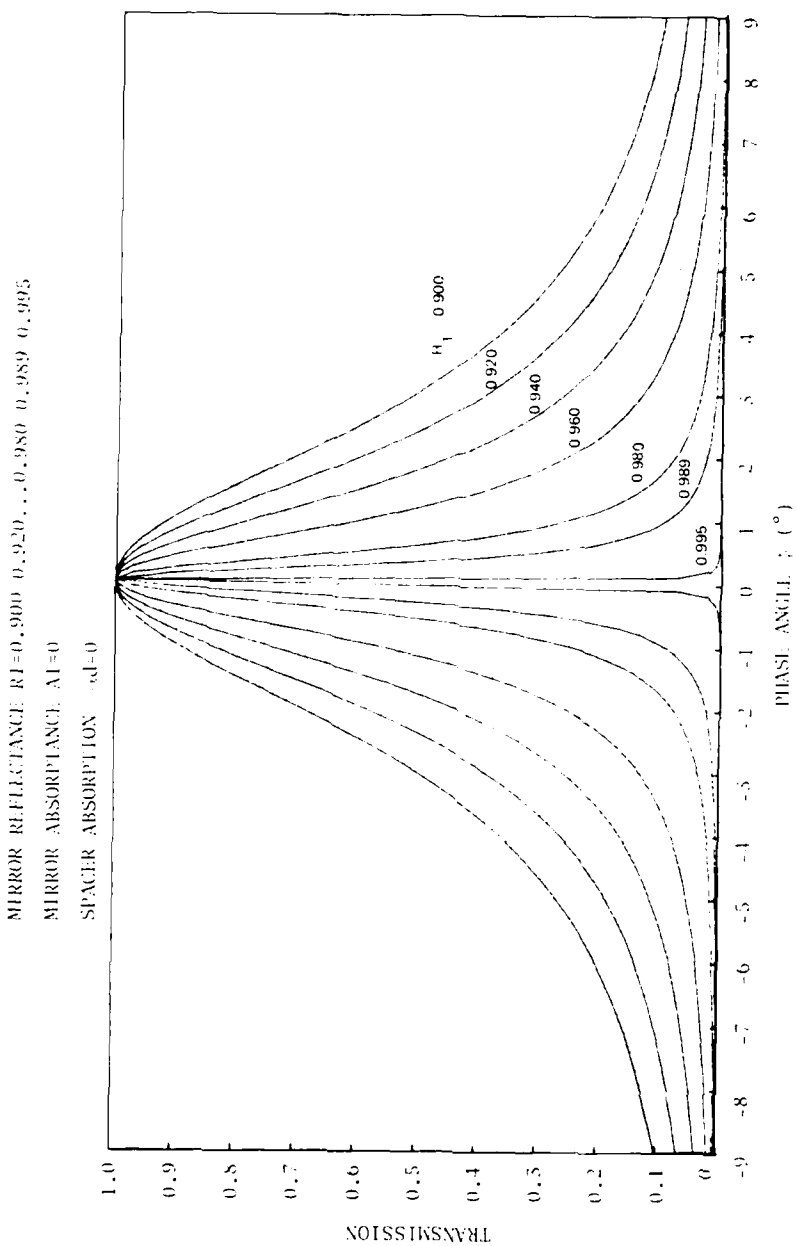

Figure 6. Effect on transmission of variable reflectance R_1, when there is no absorption in either the spacer layer or the mirrors (R_1 0.99)

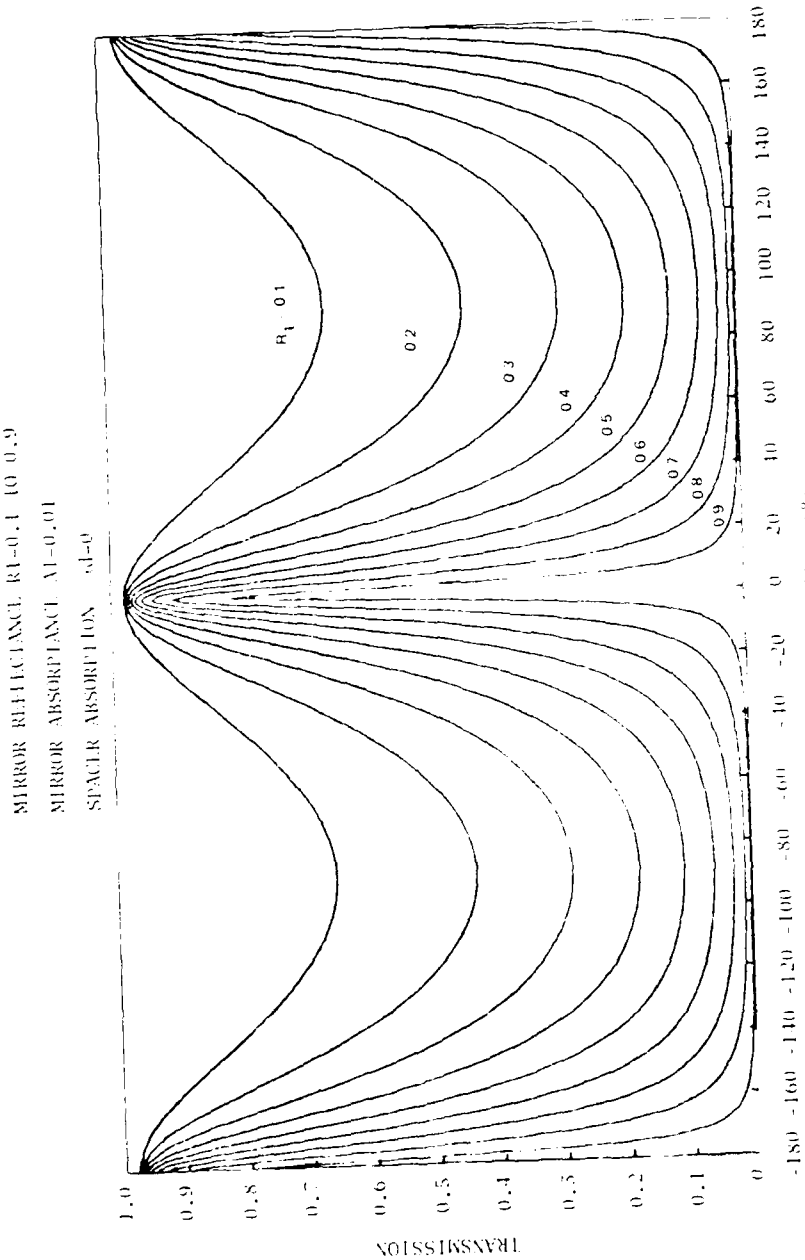

Figure 7. Effect on transmission of variable reflectance R_1, when there is no absorption in the spacer layer but a fixed absorption $A_1 = 0.01$ in both mirrors ($R_1 = 0.9$)

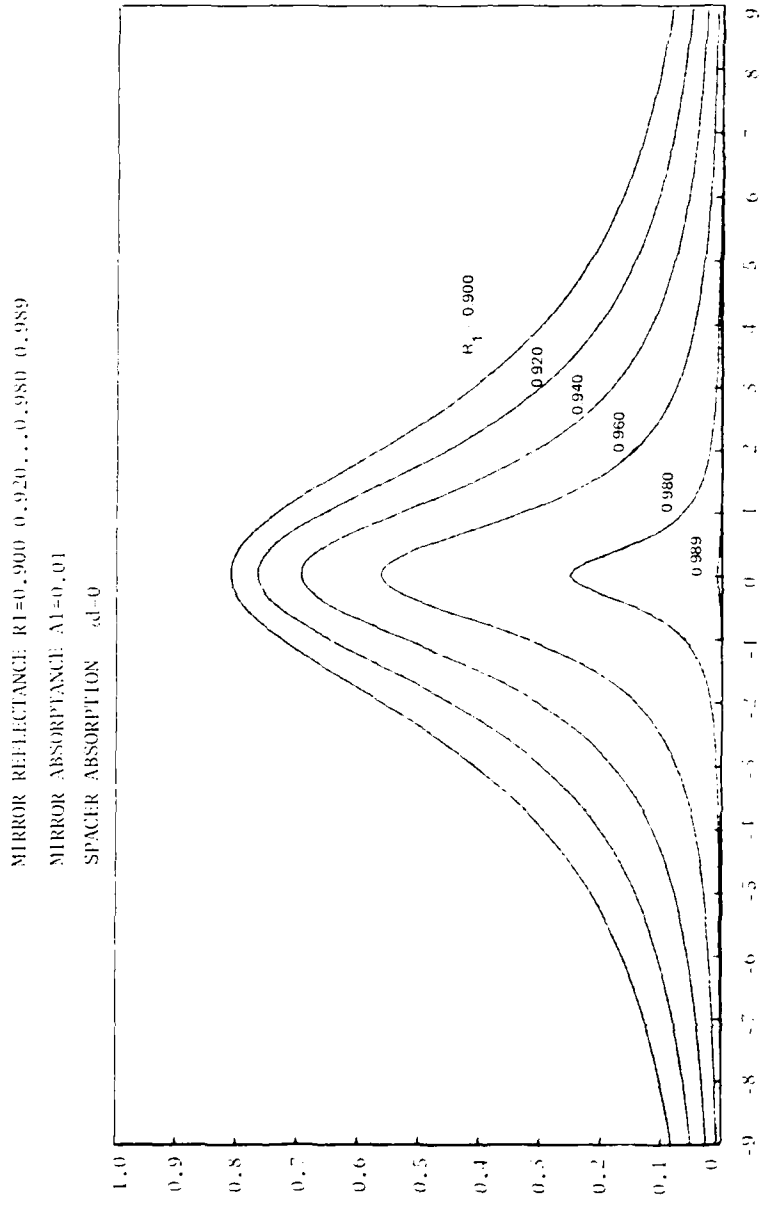

Figure 8. Effect on transmission of variable reflectance R_1, when there is no absorption in the spacer layer but a fixed absorption $A_1 = 0.01$ in both mirrors ($R_1 = 0.9$)

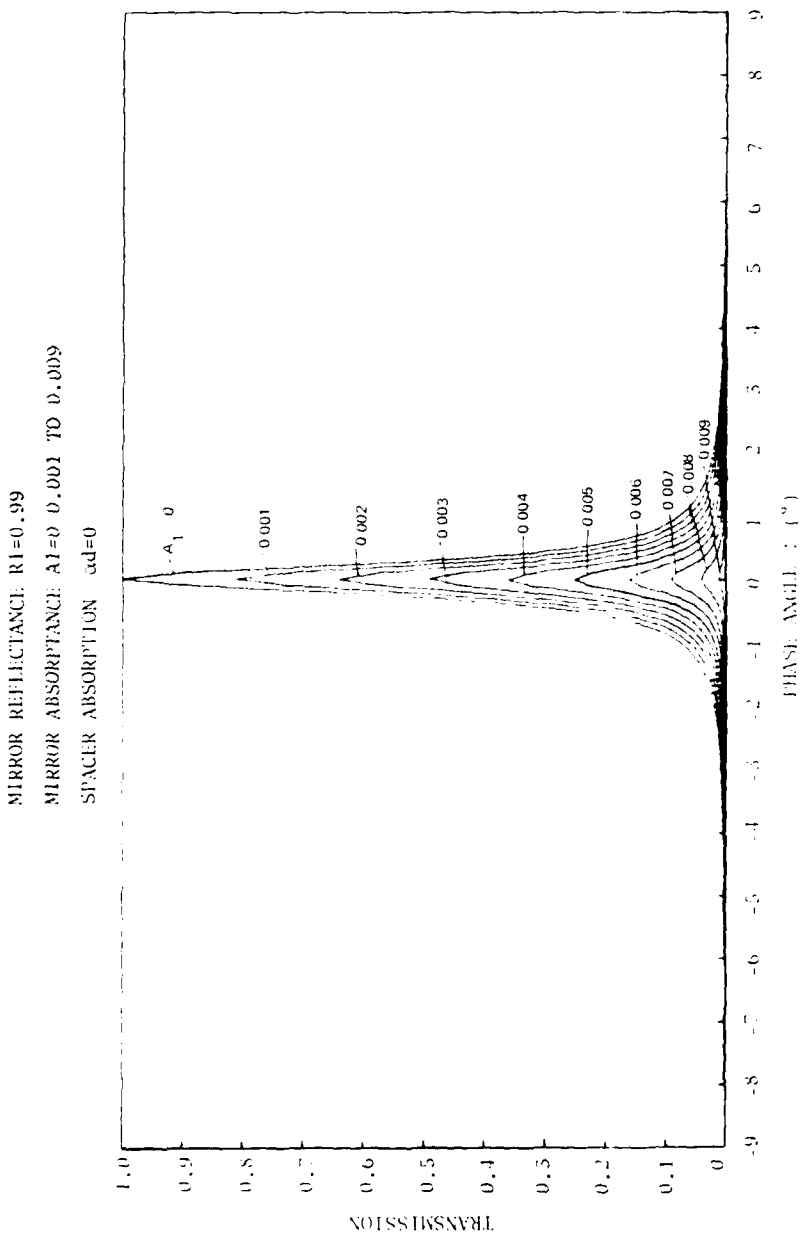

Figure 9. Effect on transmission of fixed R_1 = 0.99 and variable A_1 in the mirrors, when there is no absorption in the spacer layer

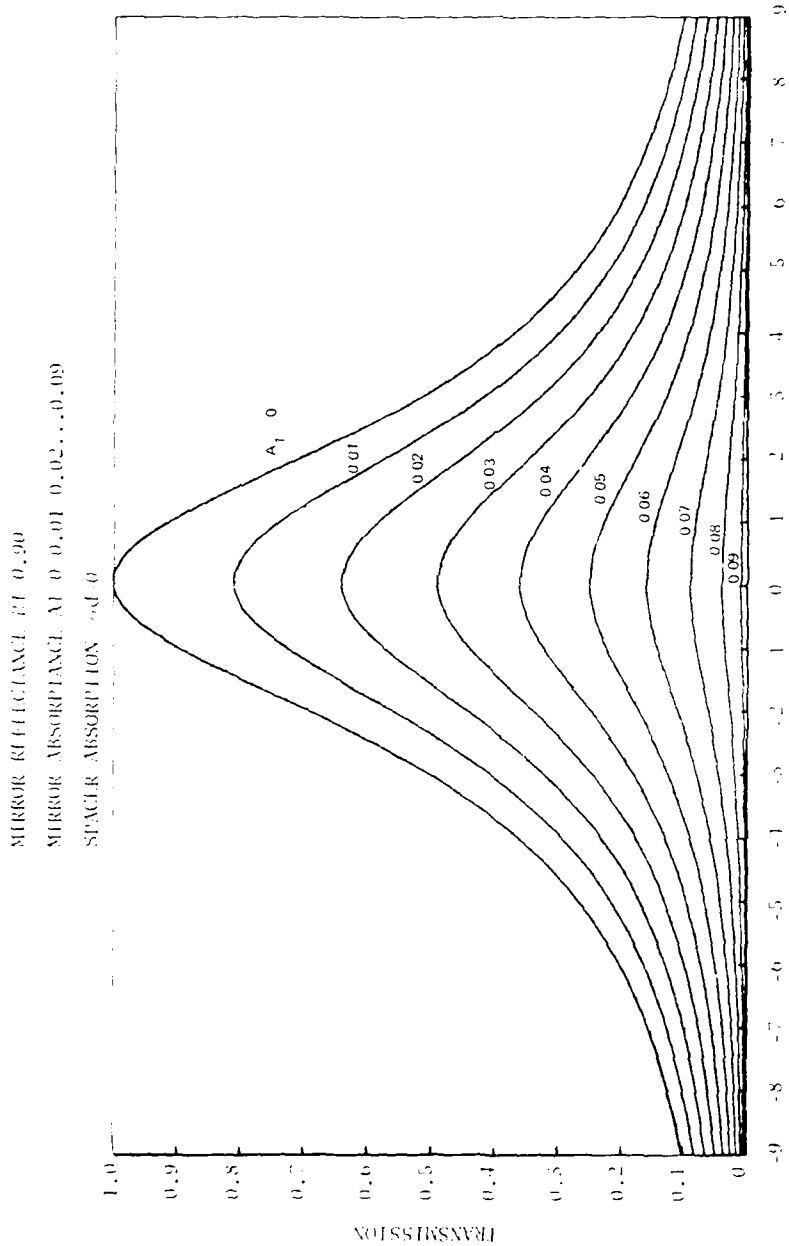

Figure 10. Effect on transmission of fixed $R_1 = 0.90$ and variable A_1 in the mirrors, when there is no absorption in the spacer layer

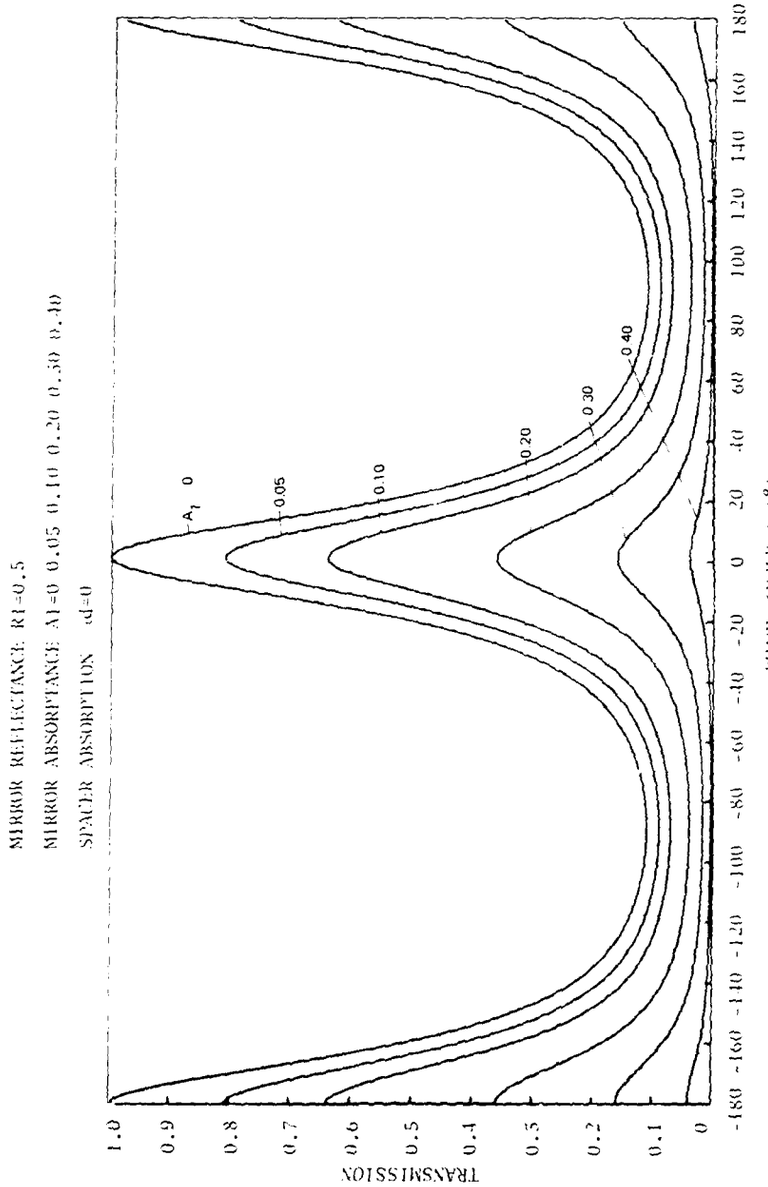

Figure 11. Effect on transmission of fixed $R_1 = 0.5$ and variable A_1 in the mirrors, when there is no absorption in the spacer layer

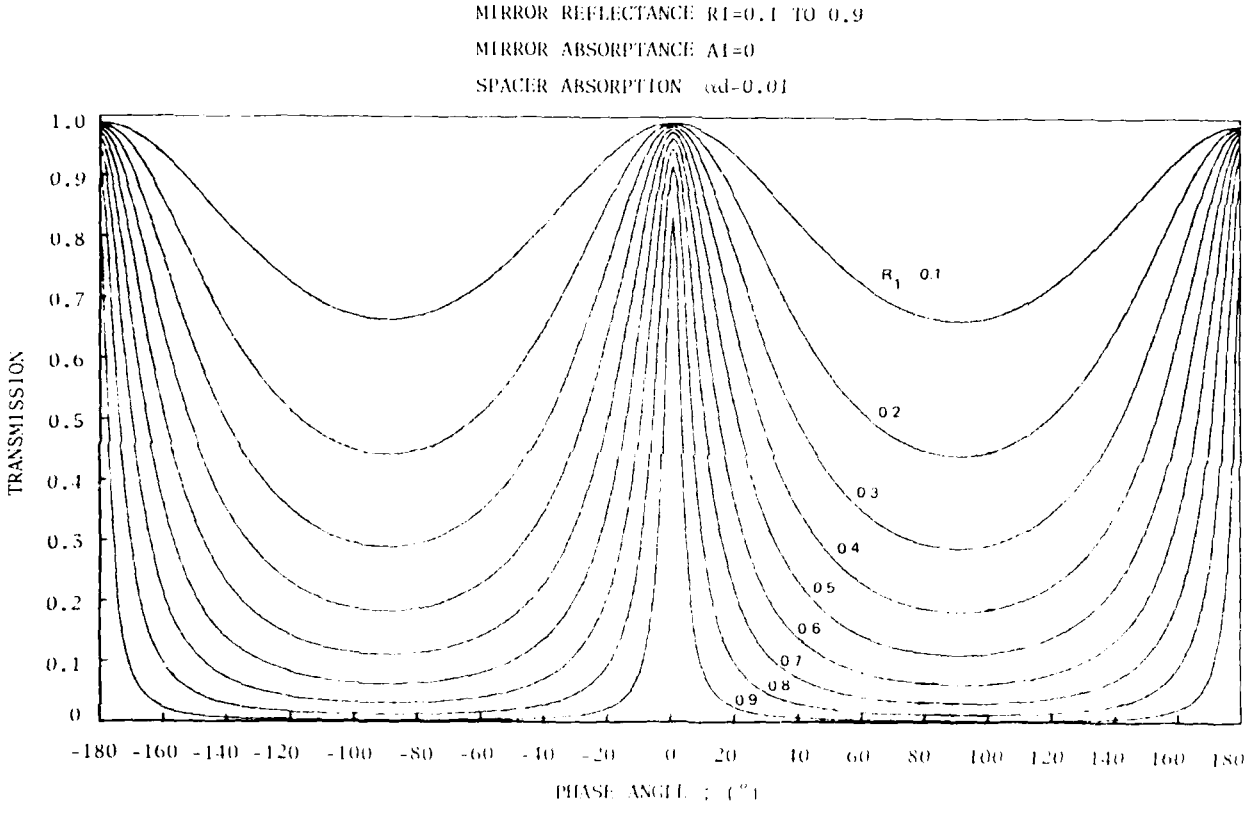

Figure 12. Effect on transmission of variable reflectance R_1 when there is no absorption in the mirrors but a fixed absorption $\alpha d = 0.01$ in the spacer layer ($R_2 = 0.90$)

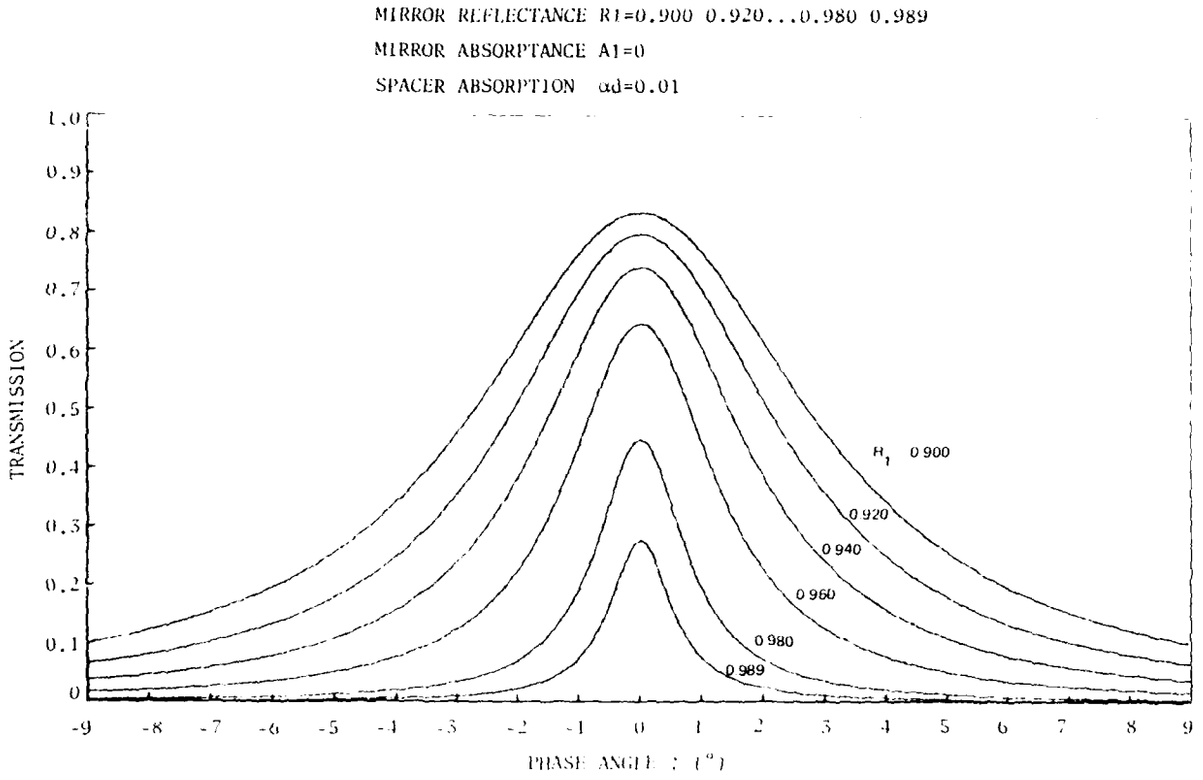

Figure 13. Effect on Transmission of variable reflectance R_1 when there is no absorption in the mirrors but a fixed absorption $\alpha d = 0.01$ in the spacer layer (R_1 = 0.90)

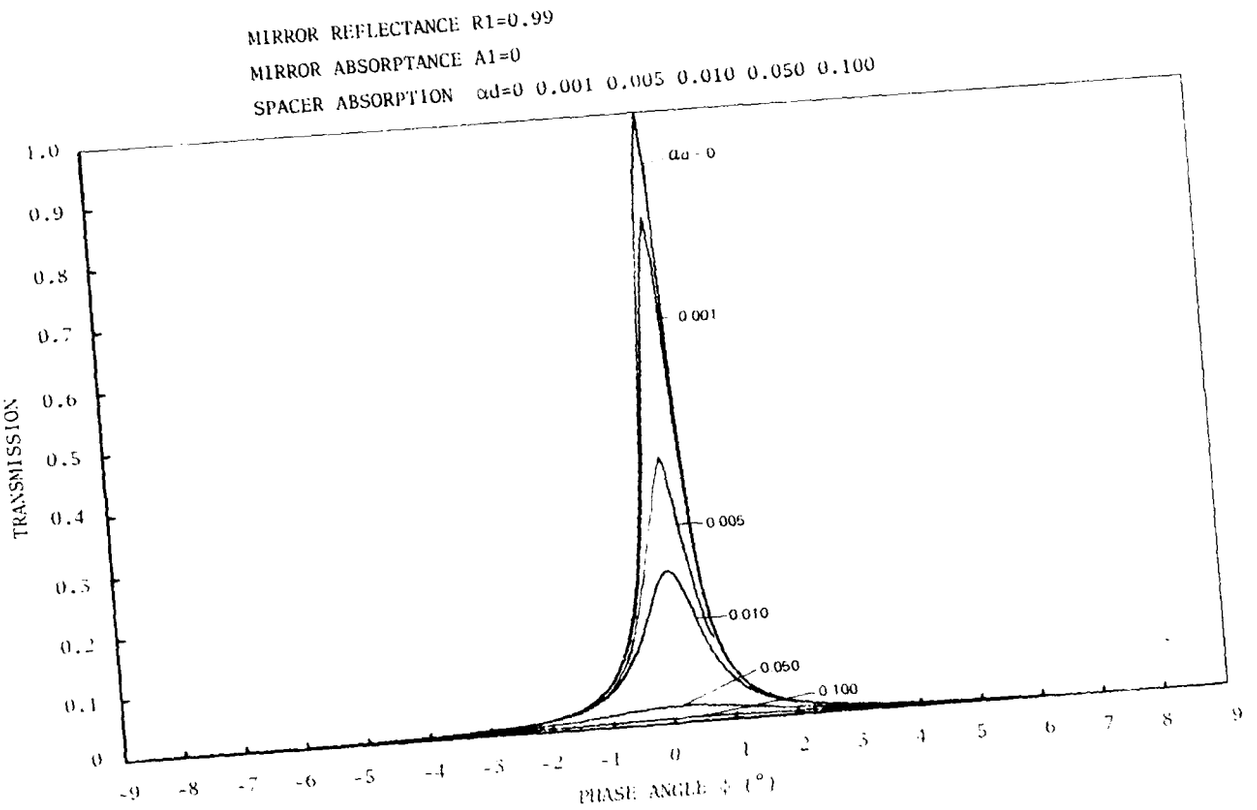

Figure 14. Effect on Transmission of fixed $R_1 = 0.99$ and variable attenuation αd in the spacer layer, when there is no absorption in the mirrors

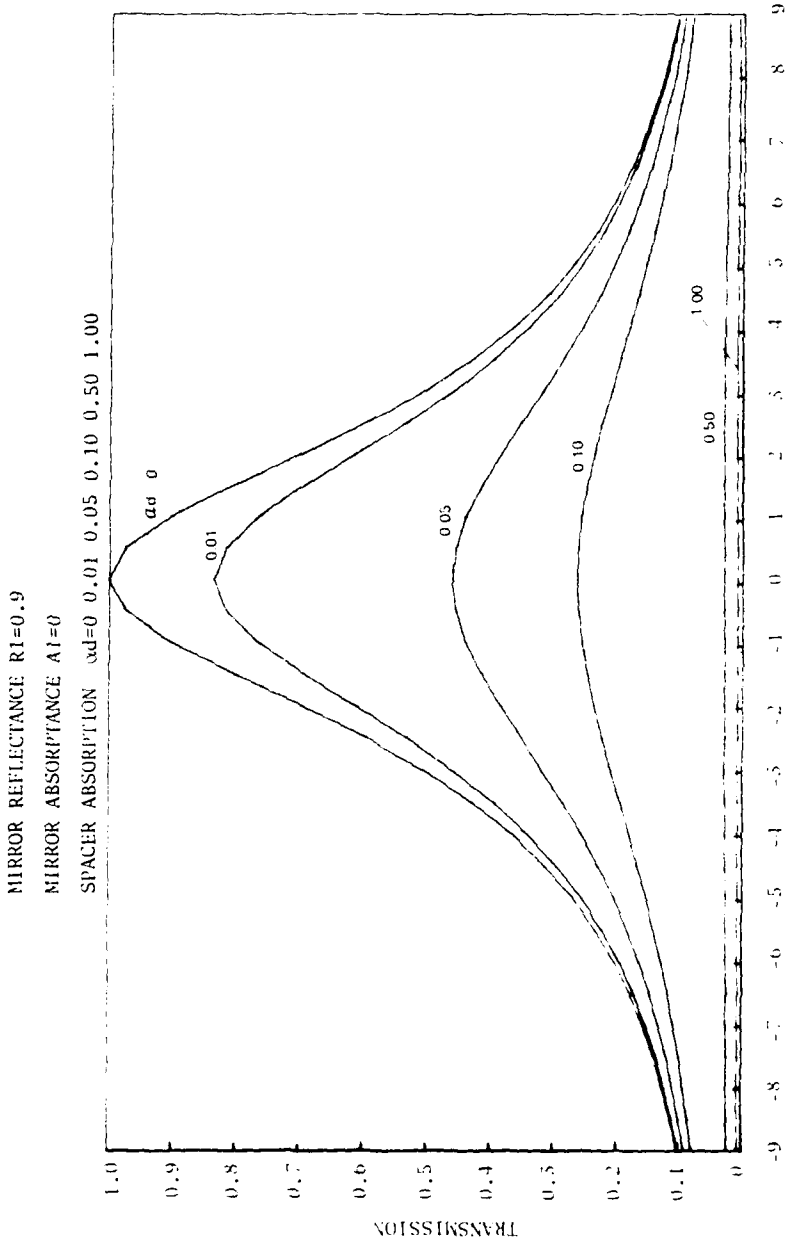

Figure 15. Effect on Transmission of fixed $R_1 = 0.90$ and variable attentuation αd in the spacer layer, when there is no absorption in the mirrors

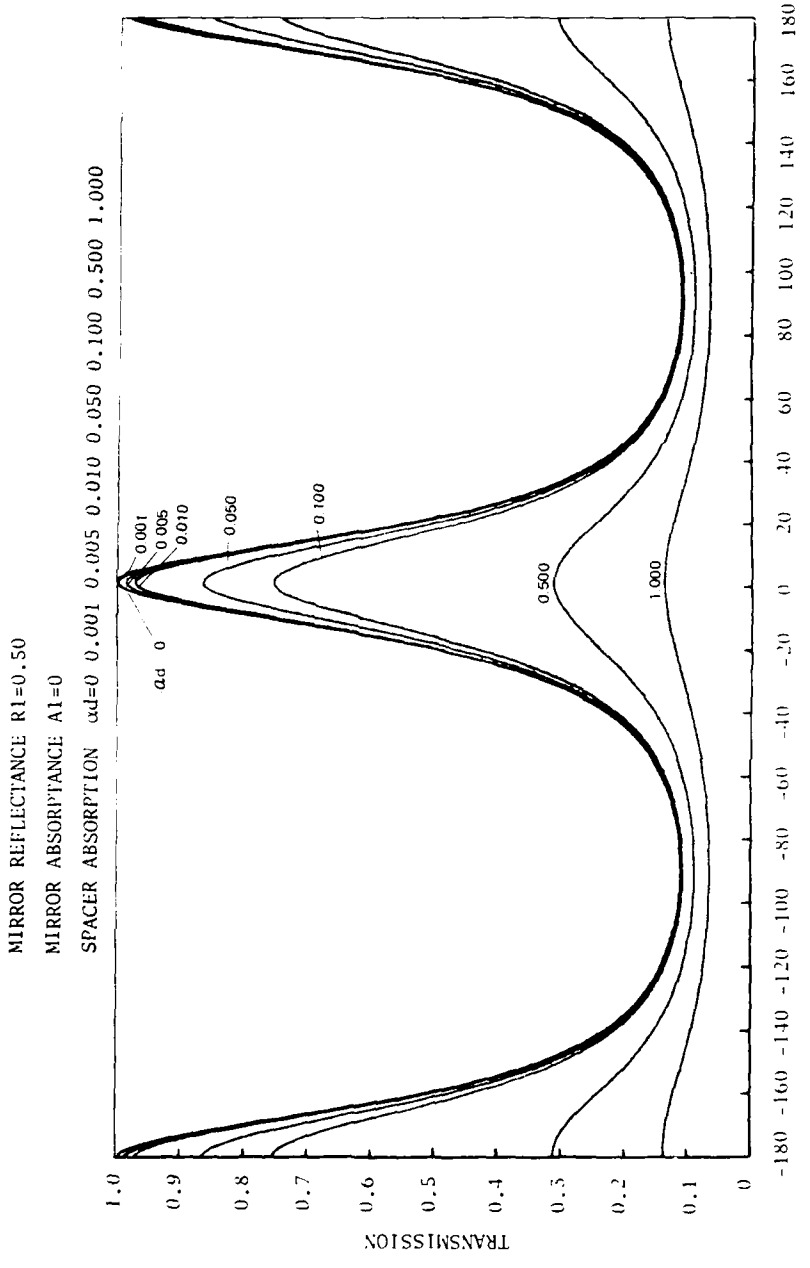

Figure 16. Effect on Transmission of Fixed $R_1 = 0.5$ and variable attenuation αd in the spacer layer, when there is no absorption in the mirrors

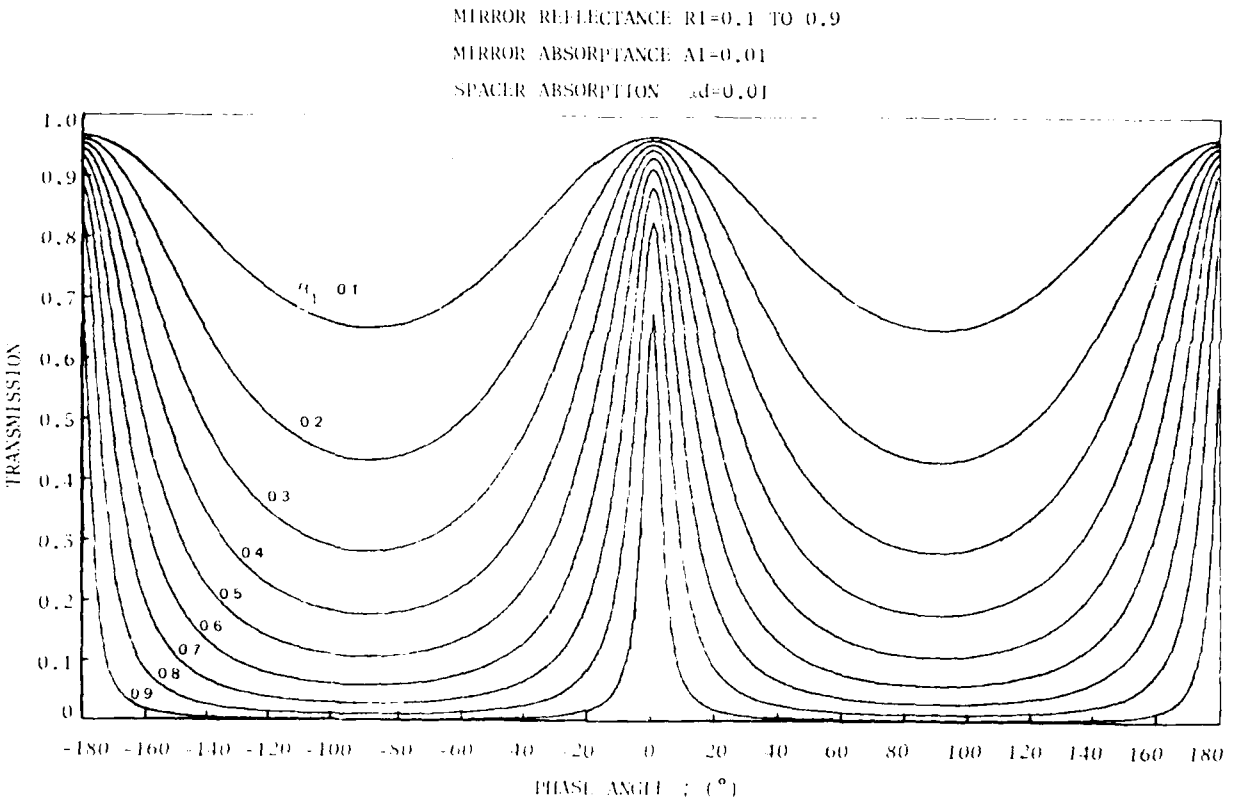

Figure 17. Effect on transmission of variable reflectance R_1 when there is fixed absorption $A_1 = 0.01$ in both mirrors and fixed attenuation $ad = 0.01$ in the spacer layer ($R_1 = 0.9$)

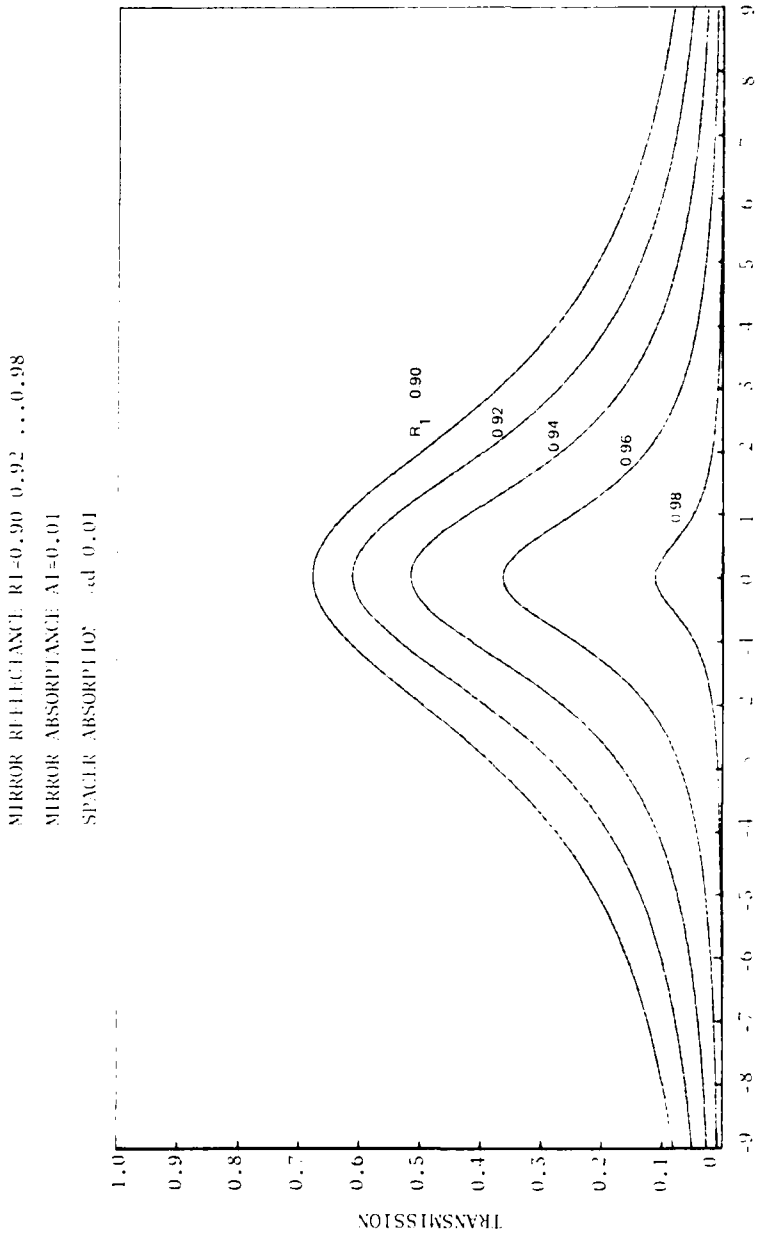

Figure 18. Effect on transmission of variable reflectance R_1 when there is fixed absorption $A_1 = 0.01$ in both mirrors and fixed attenuation $ad = 0.01$ in the spacer layer (R_1 0.9)

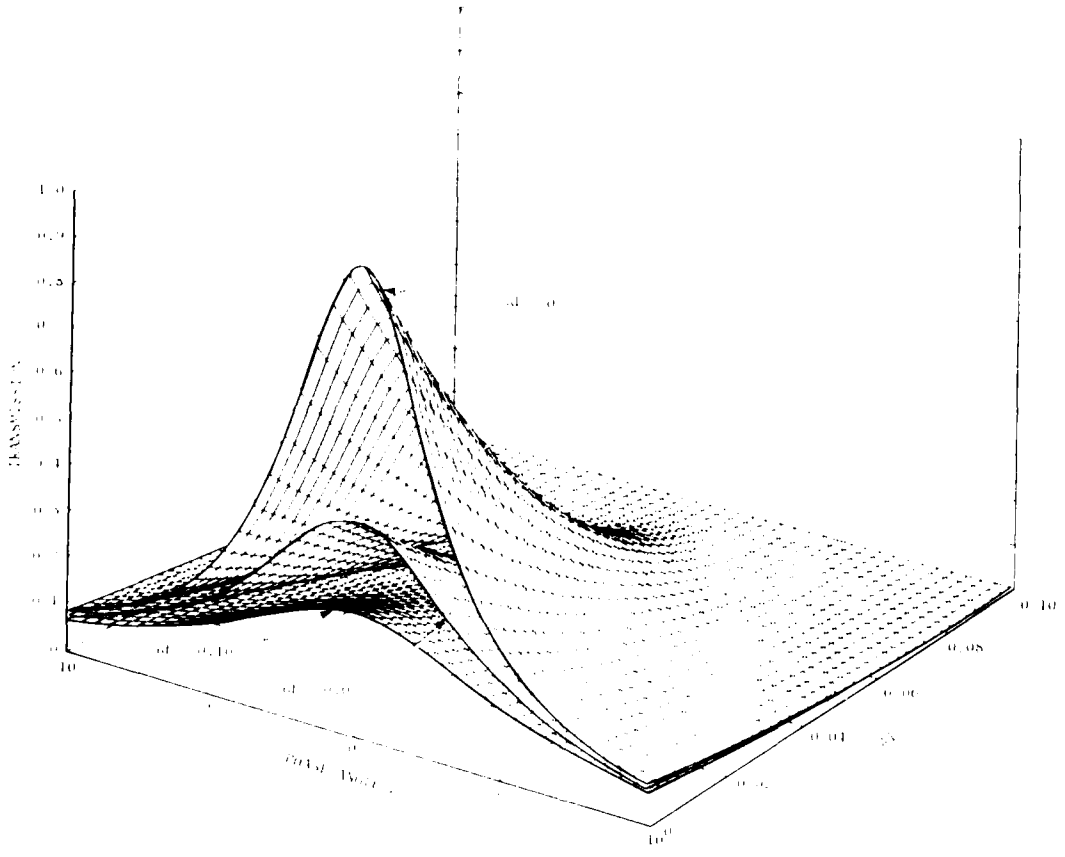

Figure 19. 3-D plot showing the effect on transmission for fixed $R_1 = 0.90$ with variable absorption A_1 in the mirrors and variable attenuation αd in the spacer layer

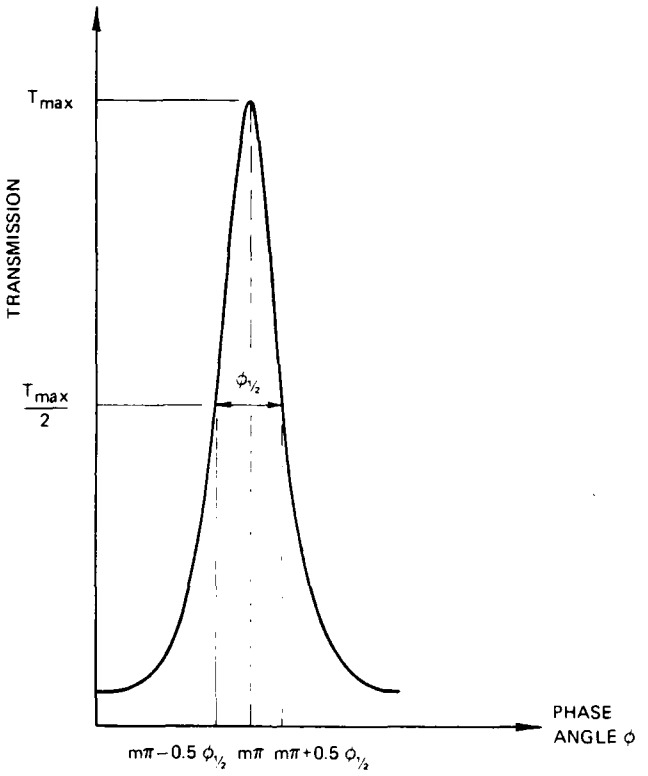

Figure 20. Definition of half bandwidth (HBW)

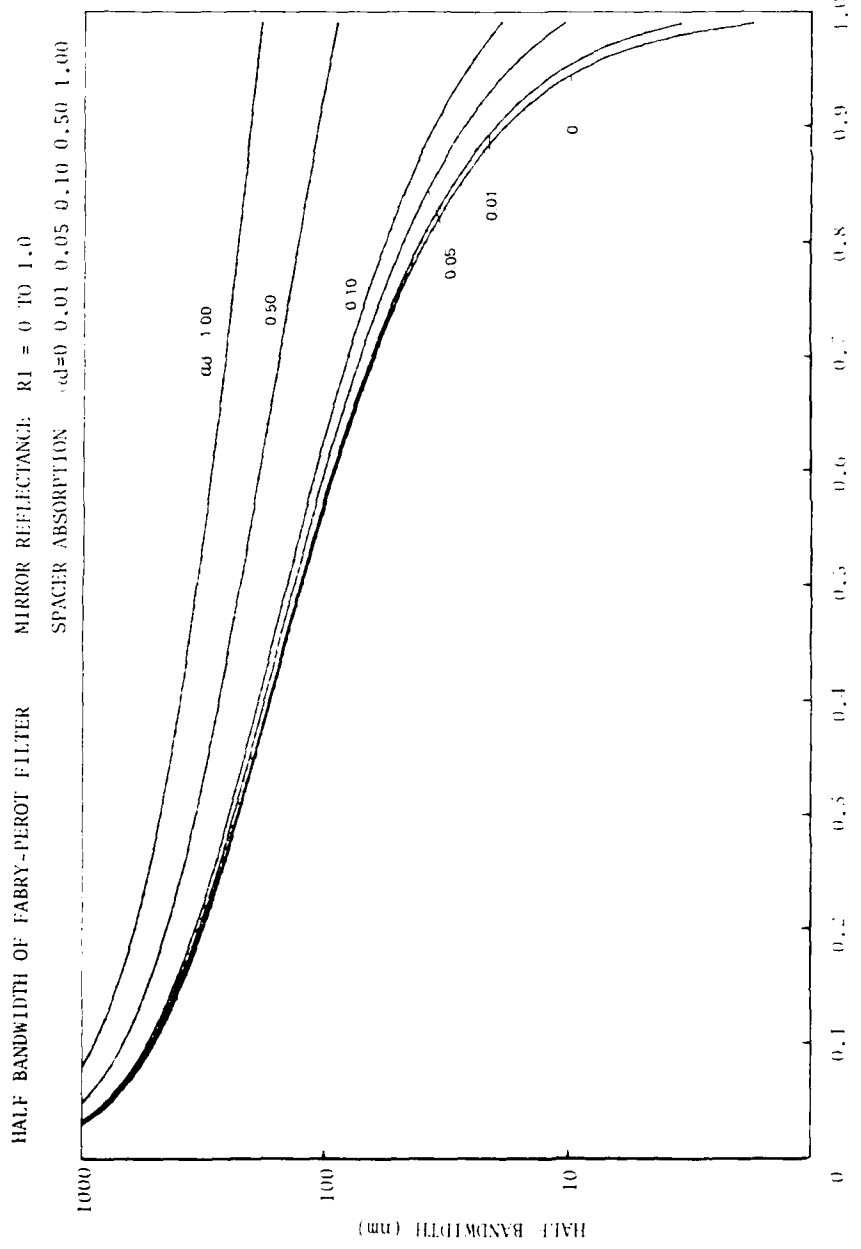

Figure 21. Effect on Half bandwidth of absorption in the spacer layer for different values of mirror reflectance

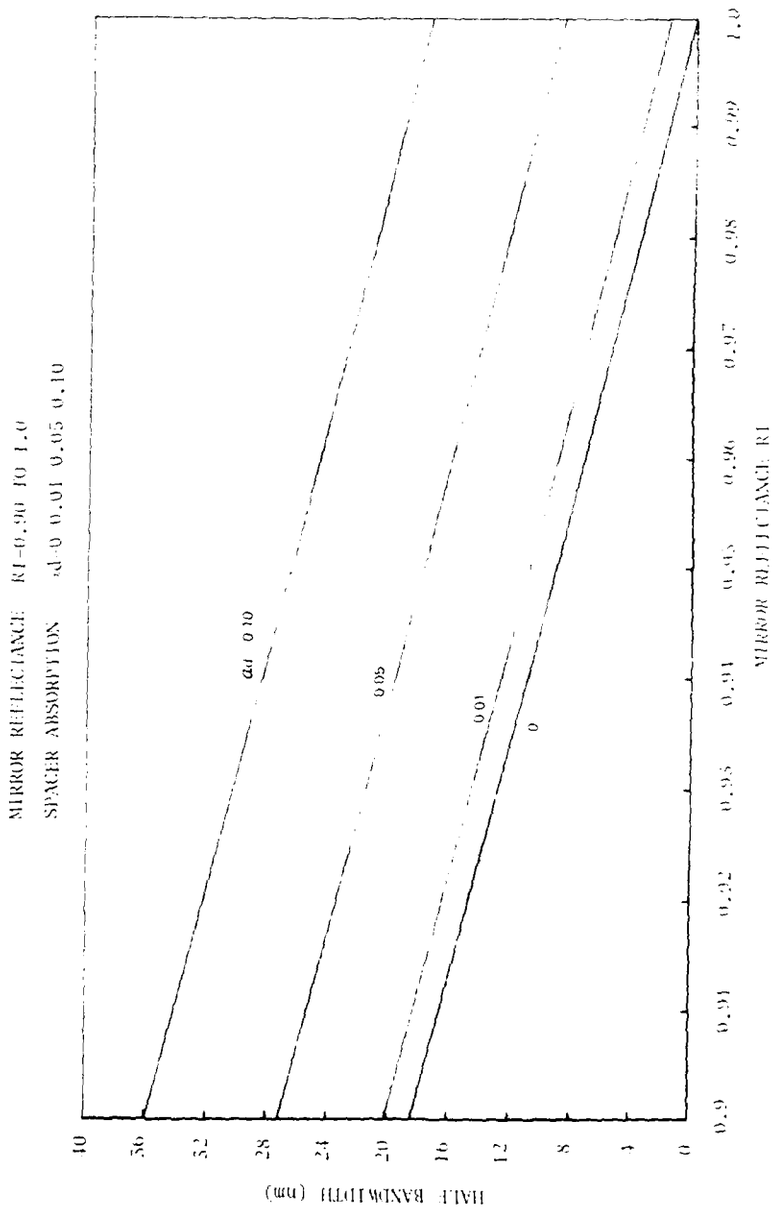

Figure 22. Effect on half bandwidth of absorption in the spacer layer for different values of mirror reflectance between 0.90 and 1.00

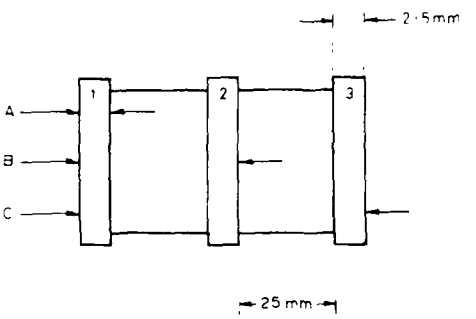

a) Plate construction

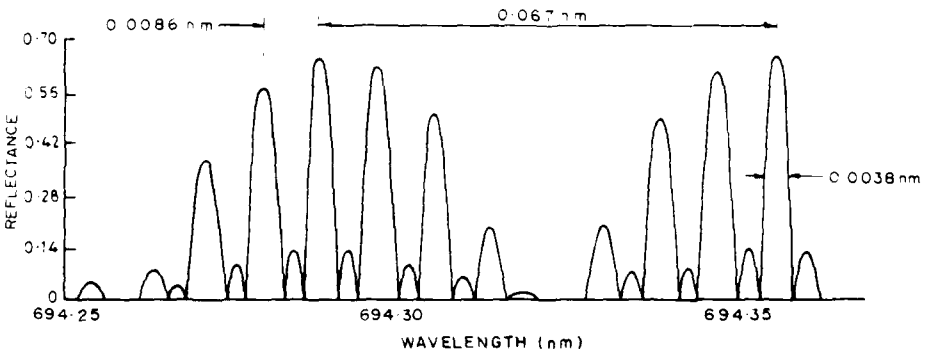

A three-plate resonant reflector

b) Reflectance versus wavelength characteristics

Figure 25. Resonant reflector curves

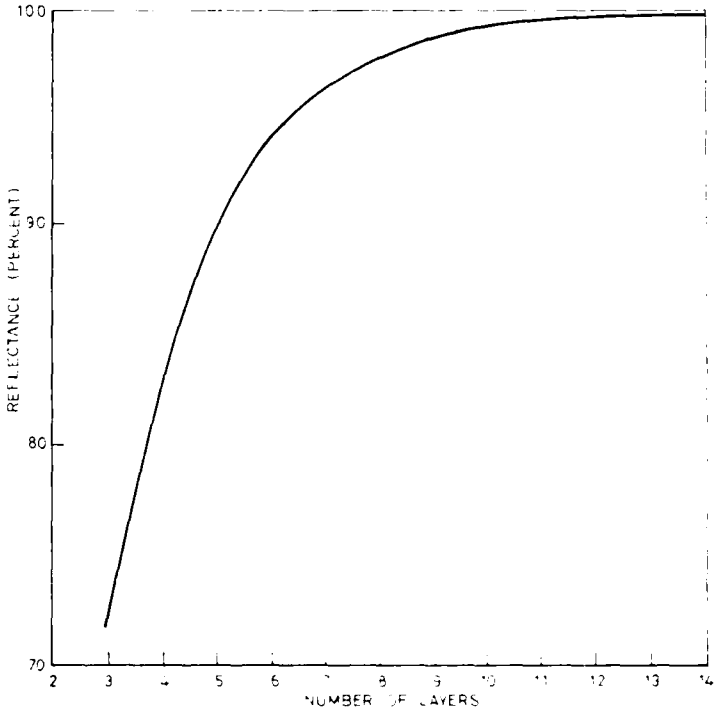

Figure 24. Reflectance versus number of layers for a Reflecting stack of quarter-wavelength thick, alternating layers of high and low reflective index

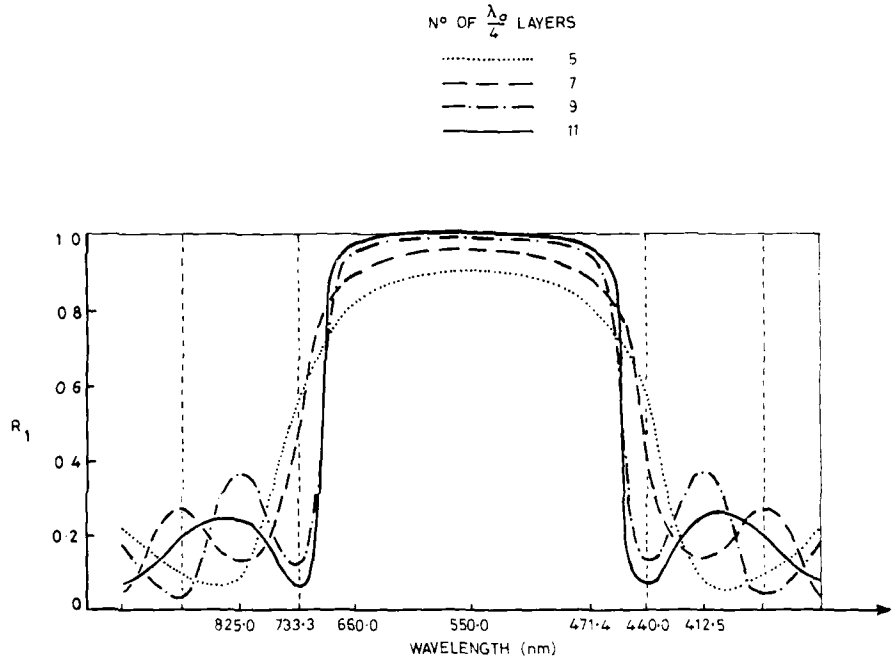

Figure 25. Reflectance versus wavelength for $\frac{\lambda_0}{4}$ multilayers of zinc sulphide and cryolite (λ_0 = 550 nm)

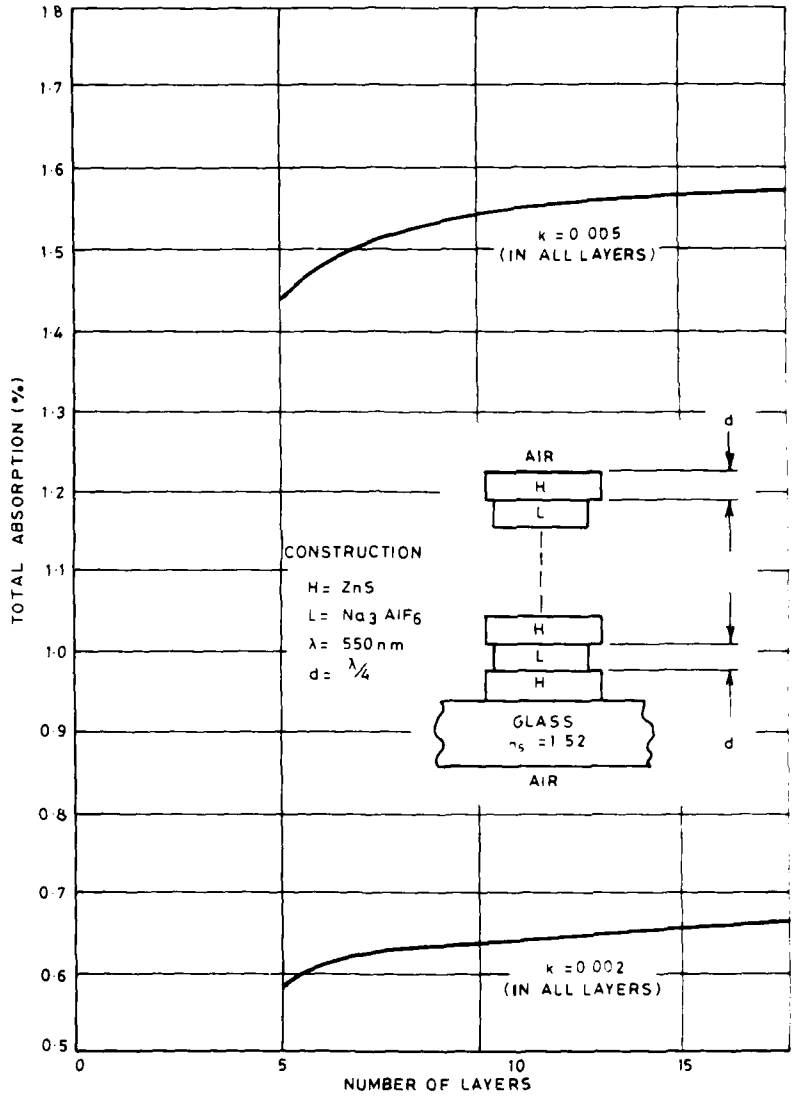

Figure 26. Effect of number of layers of absorbing materials on the total absorption in a reflecting stack of layers

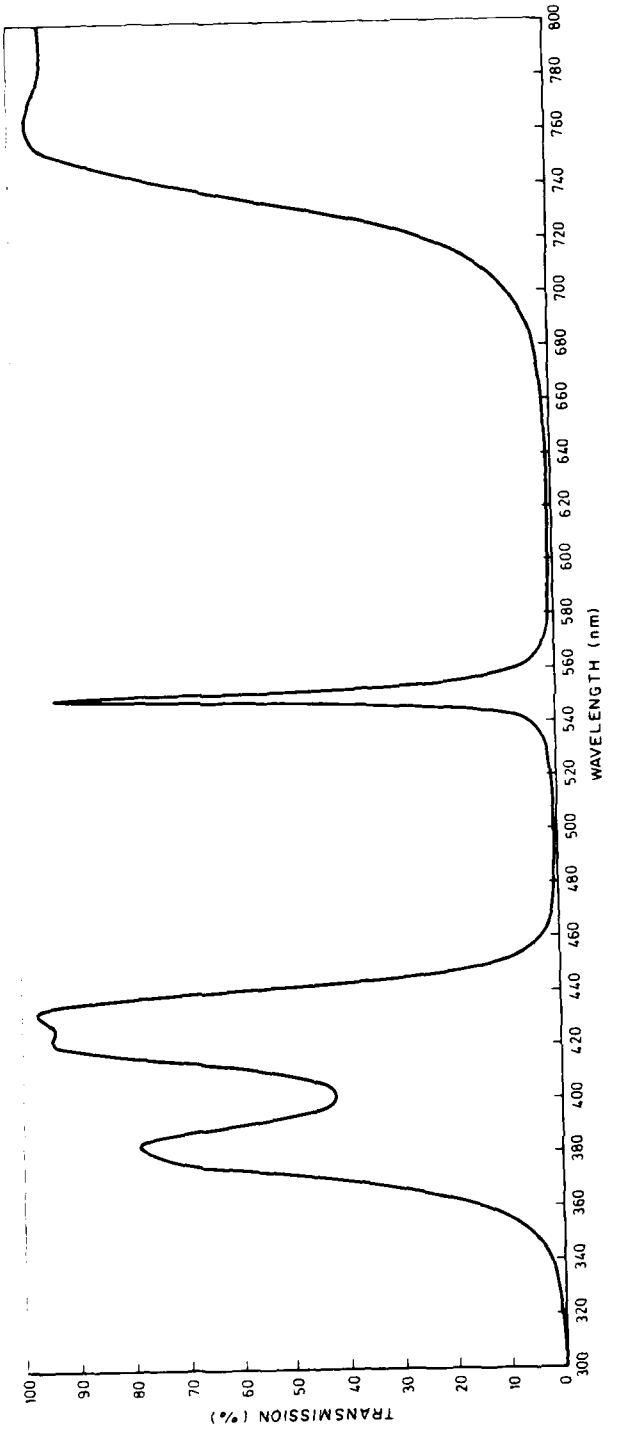

Figure 27. Transmission versus wavelength for typical Fabry-Perot filter showing sidebands

Construction	HBW (nm)
11-2L-11	0.233
11-4L-11	0.164
11-6L-11	0.127
11-8L-11	0.103

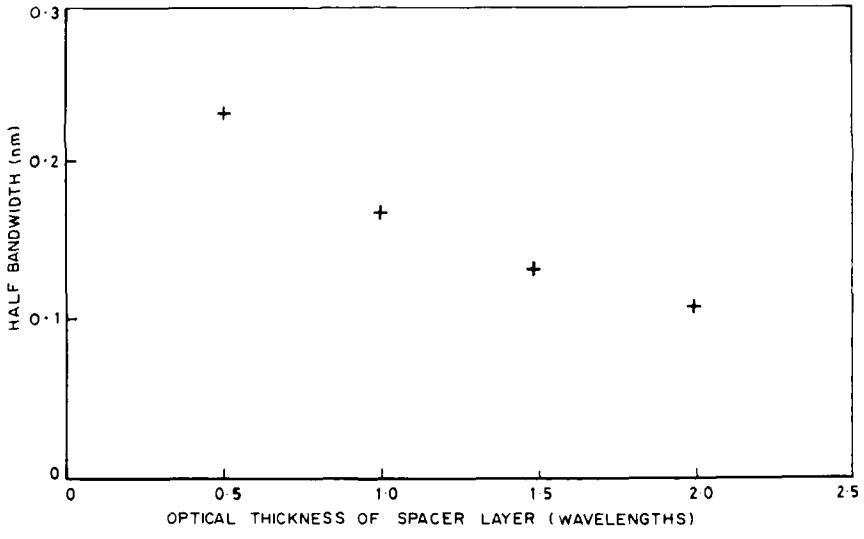

Figure 28. Effect of spacer layer thickness on half bandwidth

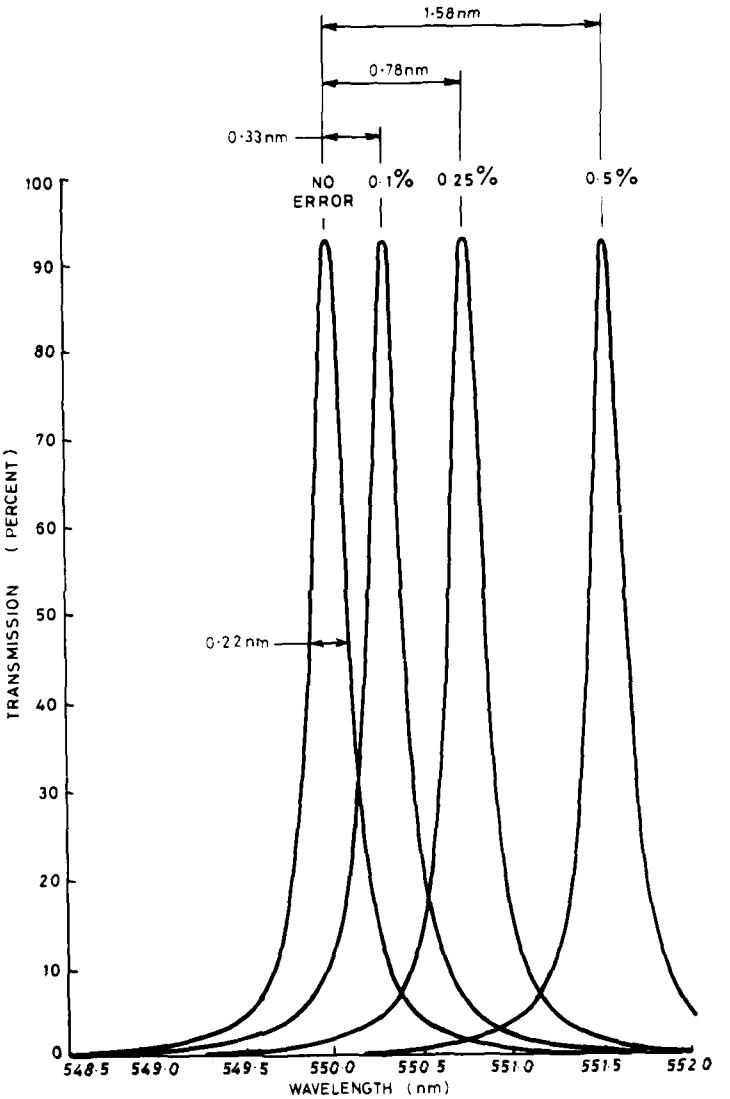

Figure 29. Effect on passband location of ab' .ily introduced errors in the spacer layer

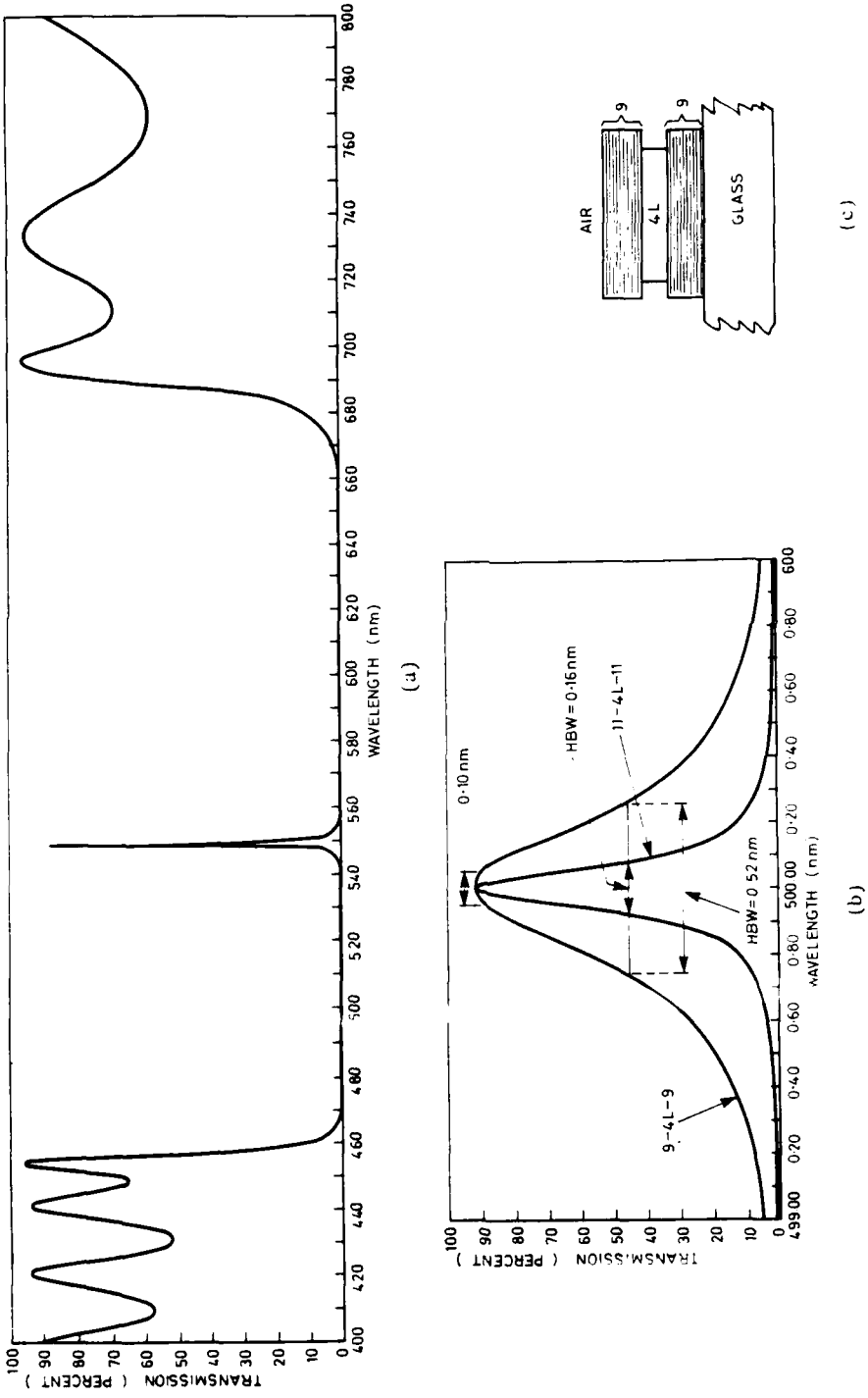

Figure 30. Transmission versus wavelength characteristics for 9-4L-9 and 11-4L-11 filters (on glass substrates, coated on one side only)

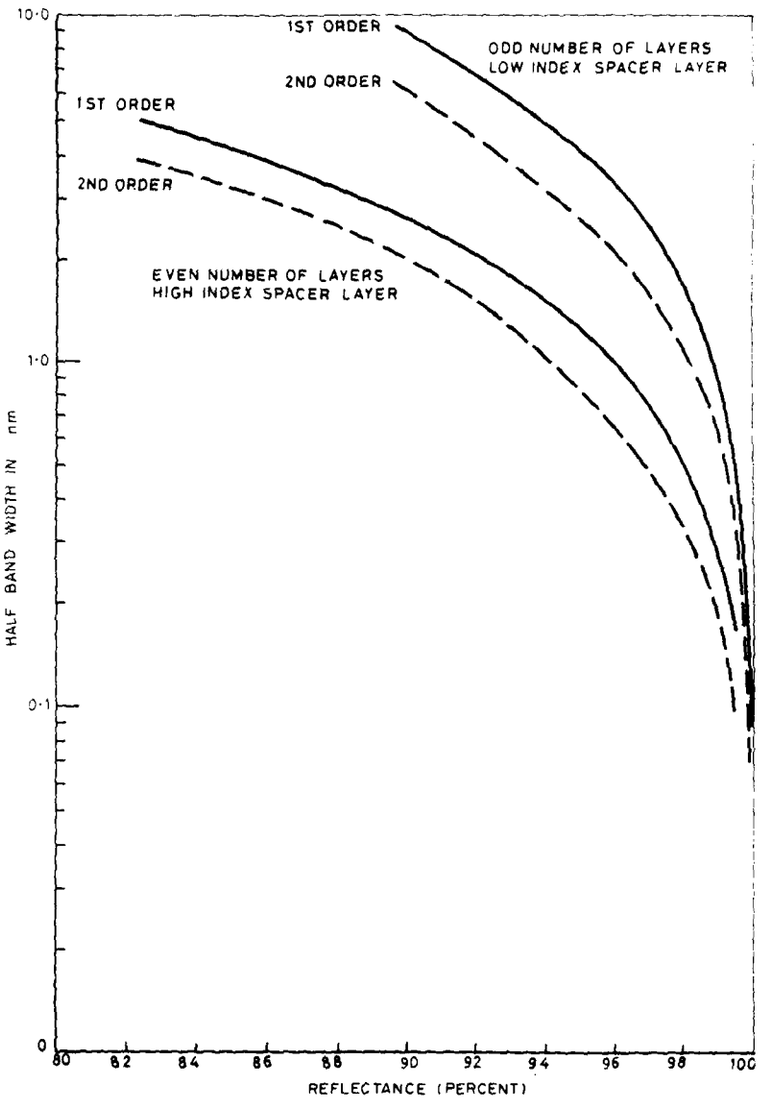

Figure 31. General trend of decreasing bandwidth with increasing reflectance for a variety of filter constructions

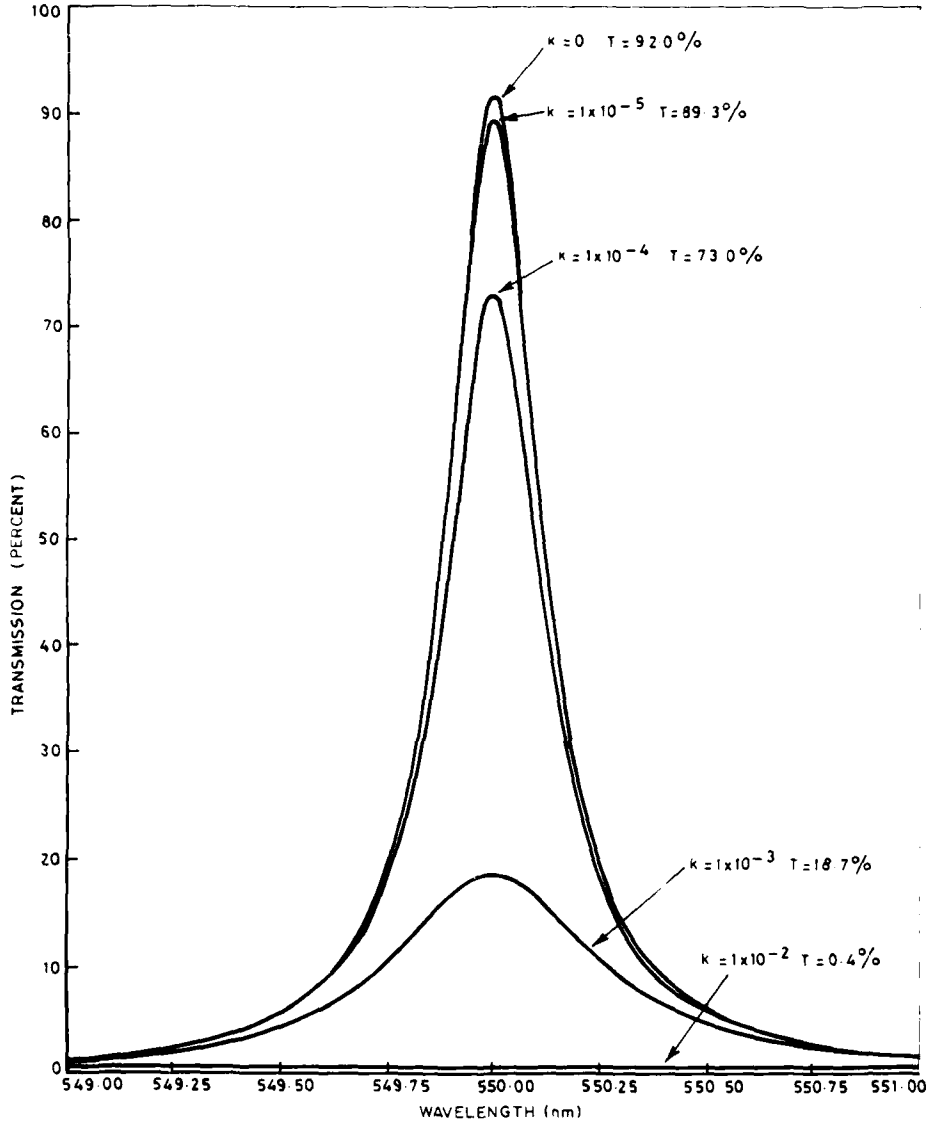

Figure 32. Effect on transmission peak of an 11-4L-11 filter which has no absorption in the reflecting stacks but an absorption index k in the spacer layer

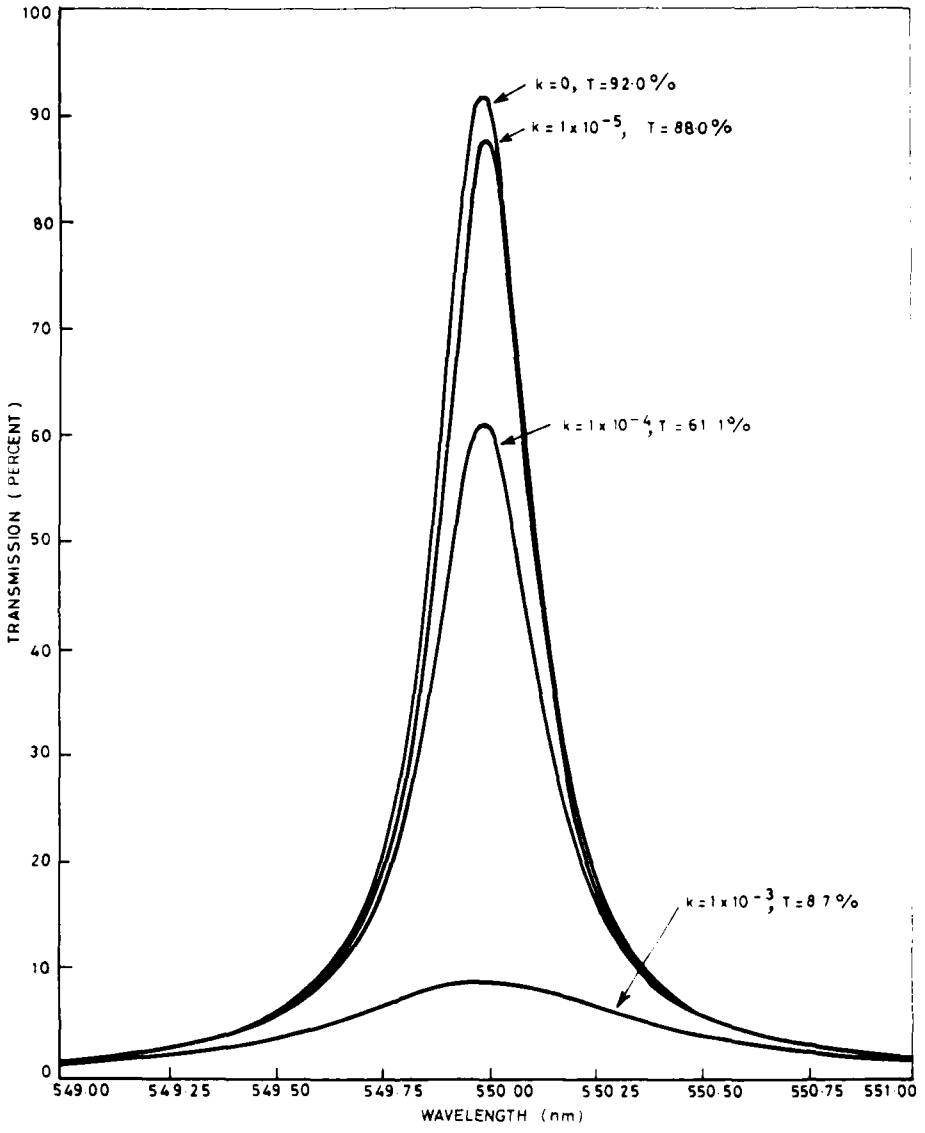

Figure 33. Effect on transmission peak of an 11-4L-11 filter which has absorption index k in every layer

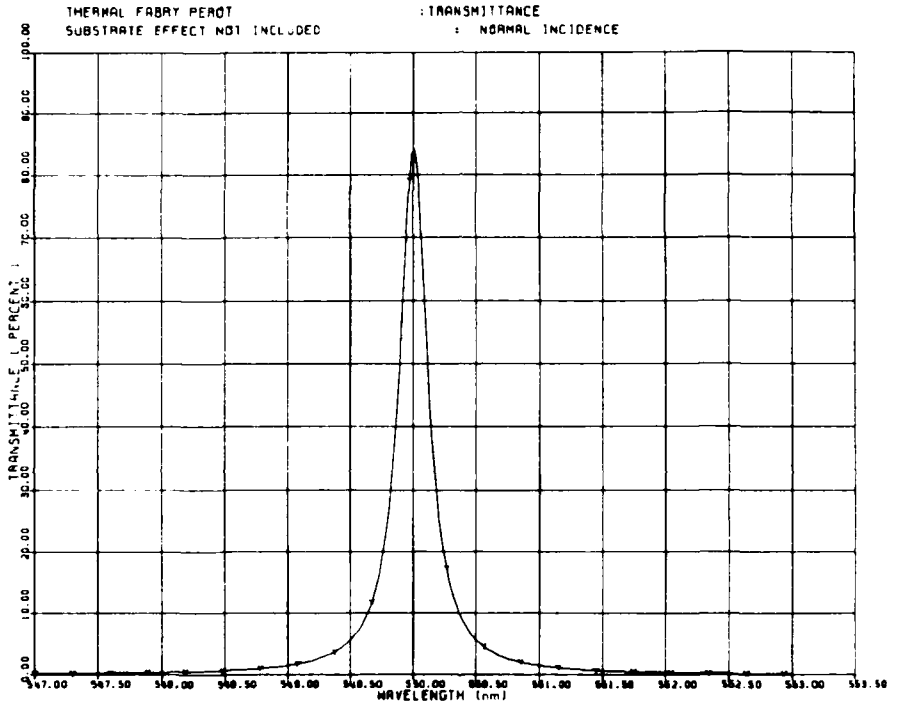

(a) Angle of incidence 0°

Figure 34. Passband shape and location for 11-4L-11 filter at various angles of incidence in parallel light (a to h)

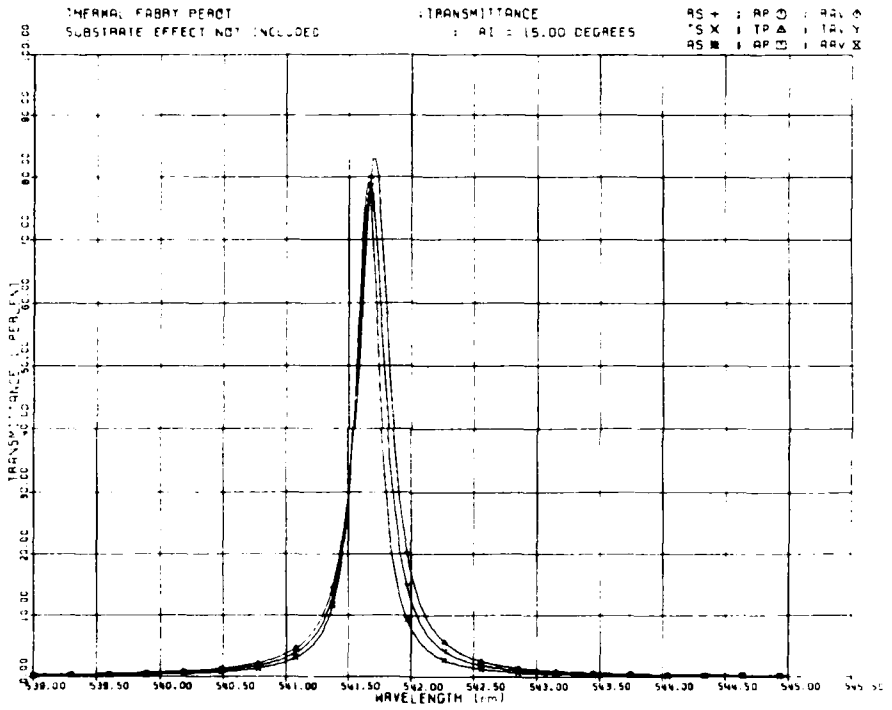

(b) Angle of incidence 15°

Figure 34(Contd.).

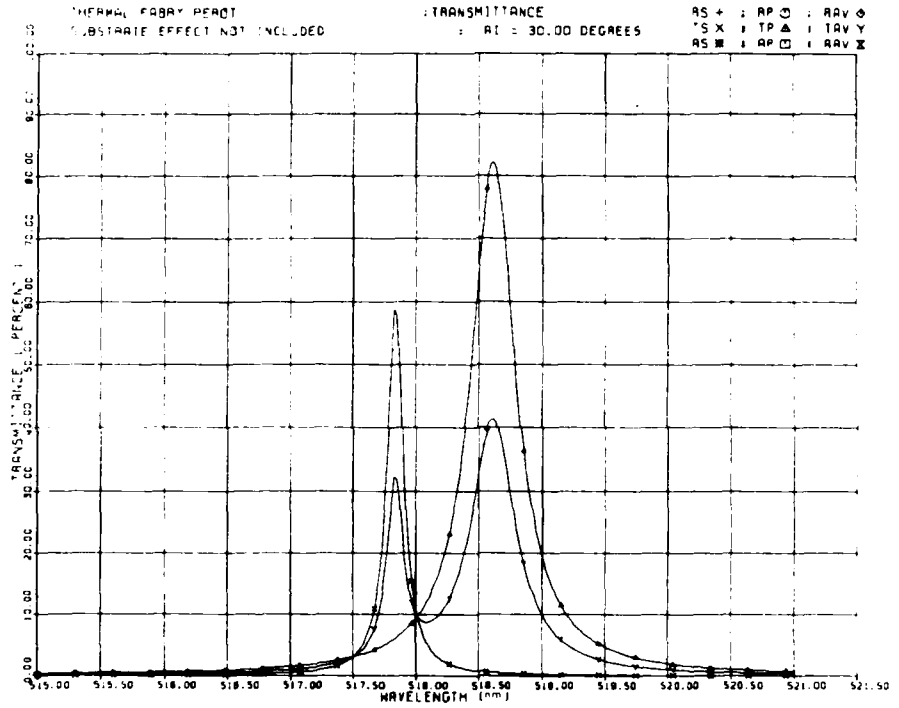

(c) Angle of incidence 30°

Figure 34(Contd.).

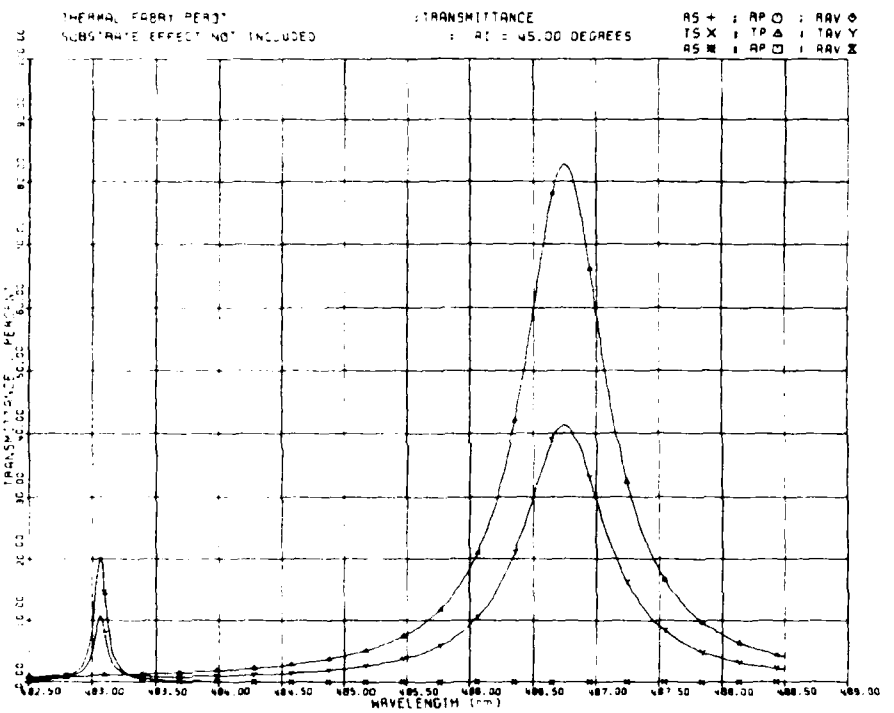

(d) Angle of incidence 45°

Figure 34(Contd.).

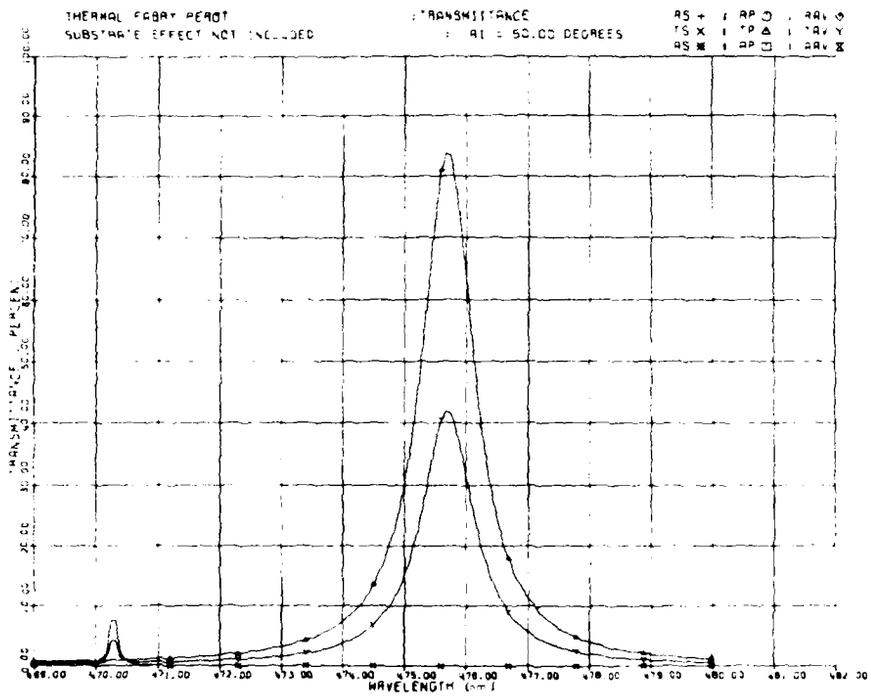

(e) Angle of incidence 50°

Figure 34(Contd.).

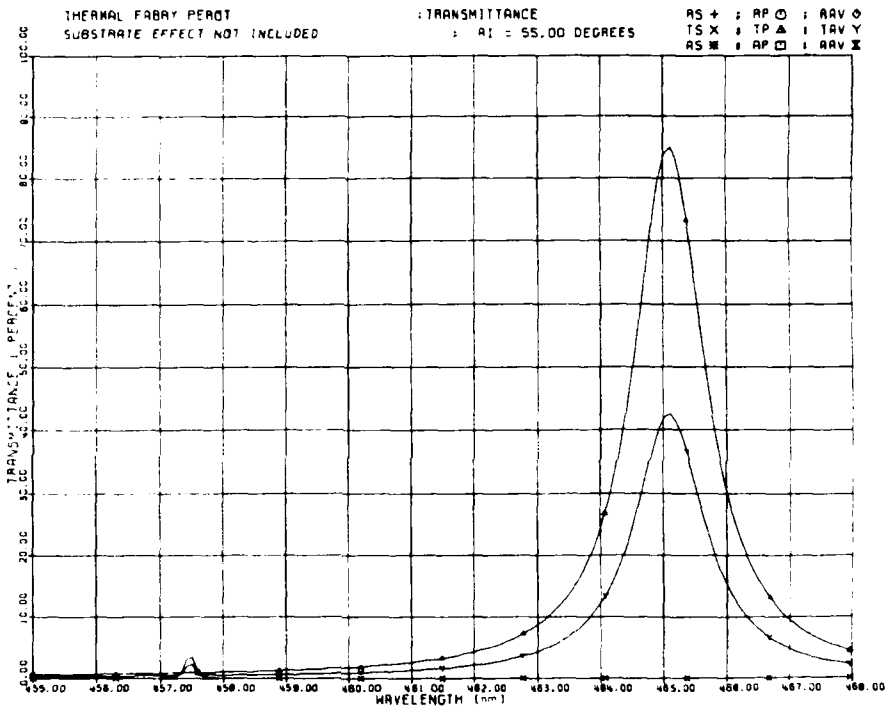

(f) Angle of incidence 55°

Figure 34(Contd.).

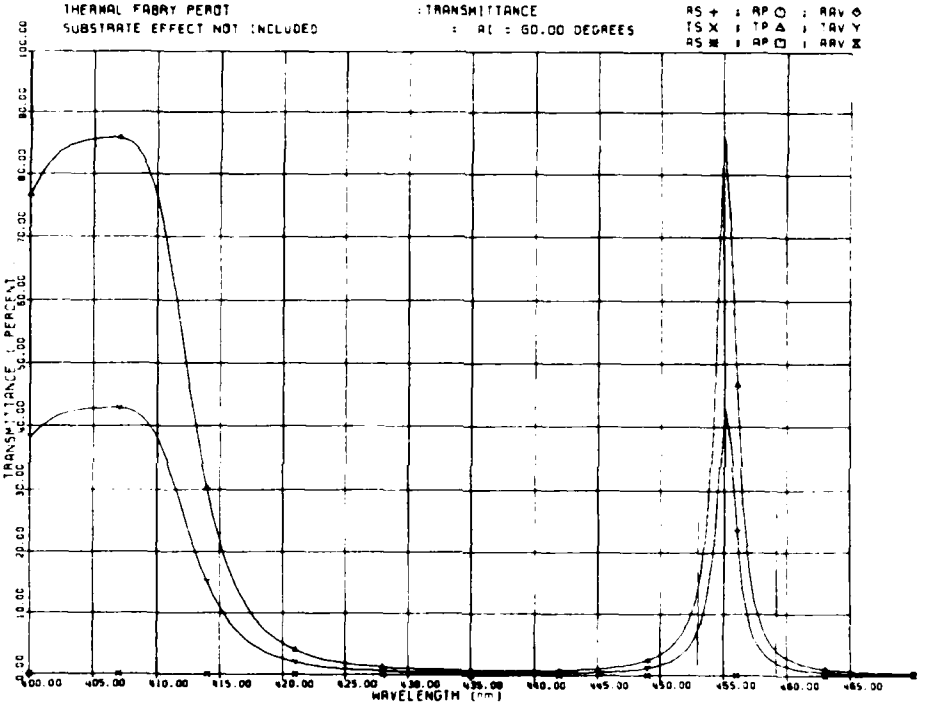

(g) Angle of incidence 60°

Figure 34(Contd.).

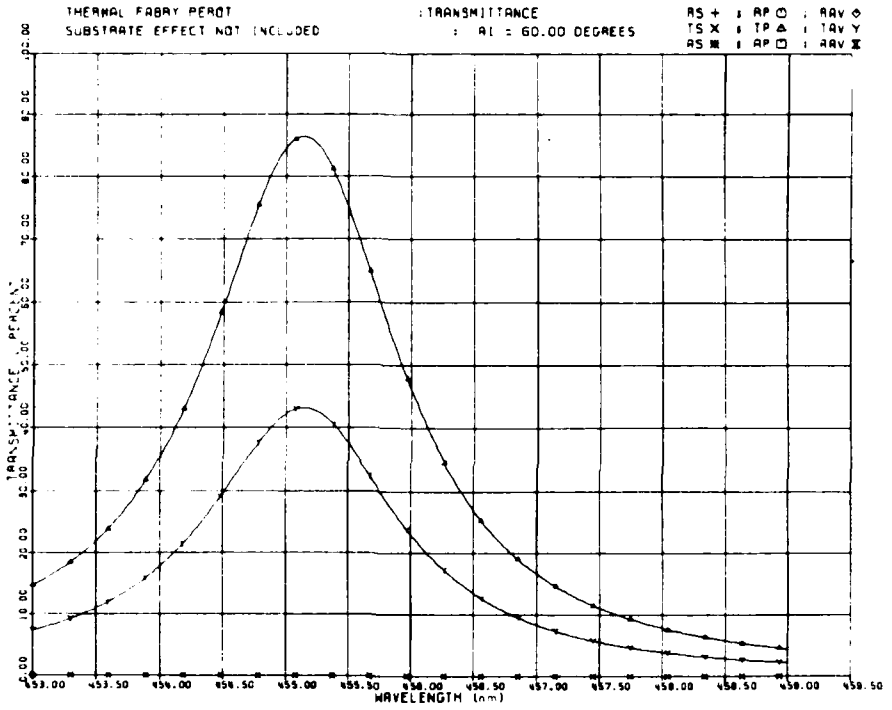

(h) Angle of incidence 60° (enlarged detail of figure 34(g))

Figure 34(Contd.).

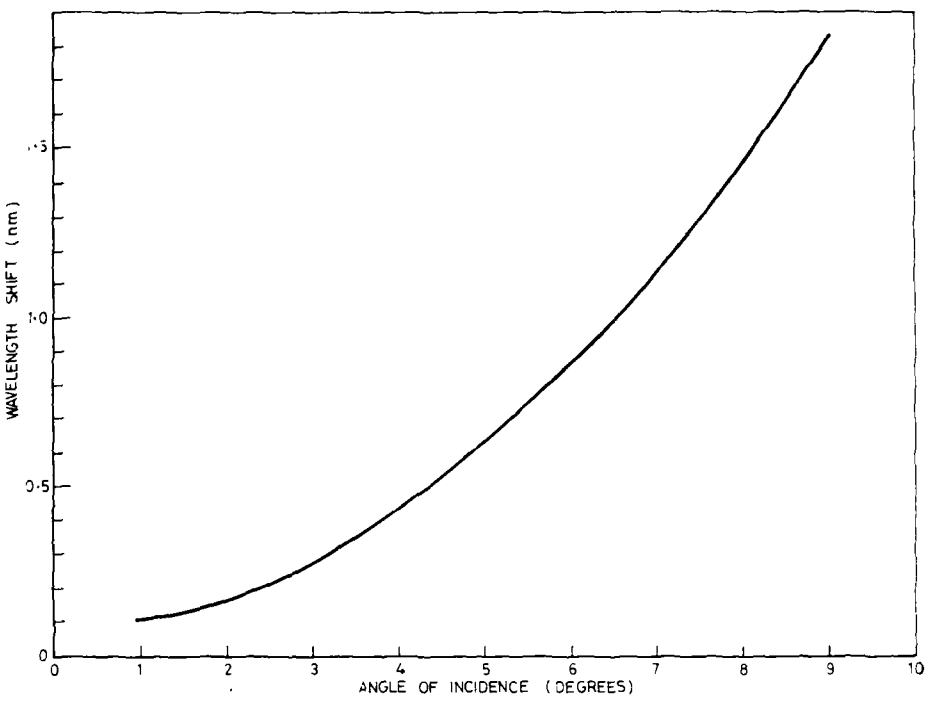

Figure 35. Shift in wavelength of peak transmission vs angle of incidence θ_i for an 11-4L-11 filter (measured in an f11 beam at 550 nm)

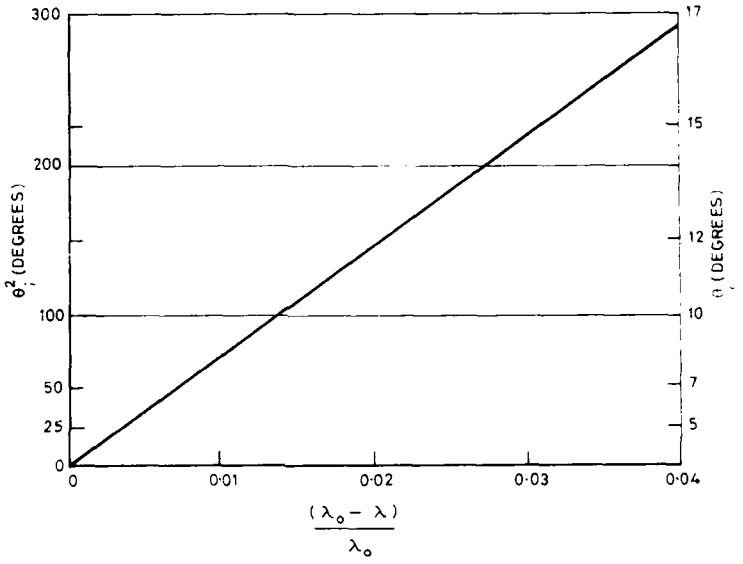

Figure 36. Effect of changes in the angle of incidence θ_i for an 11-4L-11 filter: θ_i^2 versus relative wavelength displacement $\frac{\lambda_o - \lambda}{\lambda_o}$

THIS IS A BLANK PAGE

APPENDIX I

SOME USEFUL DEFINITIONS FOR REFLECTION AND TRANSMISSION

Since confusion frequently results between these quantities, they are defined below with the schematic aid of figure I.1.

REFLECTIVITY (denoted by R_1 in figure I.1) is the fraction of the incident radiant energy which is reflected from an optically perfect single surface (reflectivity is sometimes referred to as single surface reflectance).

REFLECTANCE (denoted by R in figure I.1) includes radiation that has been transmitted through the first surface and reflected back from the second surface.

TRANSMISSIVITY (denoted by T_1 in figure I.1) is the fraction of the incident radiant energy which is transmitted through an optically perfect single surface (transmissity is sometimes referred to as single surface transmittance).

INTERNAL TRANSMITTANCE (denoted by τ in figure I.1) is the ratio of the radiant energy that reaches the internal second surface of the medium to the radiation that departed from the internal first surface.

Internal transmittance is a property of the medium itself, and no surfaces are involved. The internal transmittance is unity unless absorption occurs within the medium. Scattering is not considered here.

TRANSMITTANCE (denoted by T in figure I.1) is the fraction of the incident radiant energy that emerges from the sample.

The magnitude of the transmitted radiation differs from the incident radiation because of the additive effects of

(i) reflection at the external first surface

(ii) absorption losses within the medium

(iii) multiple reflections within the medium at the first and second interfaces which are eventually transmitted out the first surface and contribute to the total reflectance.

ABSORPTANCE (conventionally represented by the symbol A) is the ratio of the incident radiant energy that is unaccounted for by the sum of reflectance and transmittance, to the incident intensity. For the overall system,

$$A = 1 - (R + T)$$

"EQUIVALENT SURFACE"

Using the recurrence relations(ref.I.1) it is possible to replace the net reflectance, transmittance and absorptance of a system of individual layers, each exhibiting absorption and multiple internal reflections, by an "equivalent surface". The single surface reflectance R_1 of the equivalent surface is then equal to the reflectance R of the system of layers while the single surface transmittance T_1 of the equivalent surface is equal to the transmittance T of the system of layers. The concept of "equivalent surface" also includes the situation of absorption - the resultant absorptance A of a

multilayer system is then replaced by the absorption A_1 of the equivalent single surface, where now

$$A_1 = 1 - (R_1 + T_1)$$

Note: The general terms Reflection and Transmission are often used when strict nomenclature should specify Reflectance and Transmittance, or Reflectivity and Transmissivity.

The Specific terms "Reflection Coefficient r" and "Transmission Coefficient t" as defined by the Fresnel coefficients, refer to the ratios of reflected/incident and transmitted/incident amplitudes, and are related to the single surface reflectance and single surface transmittance. The Fresnel coefficients are considered in more detail in Appendix II.

REFERENCES

No.	Author	Title
I.1	Abele's, F.	Ann.d. Physique 3 504, (1948)

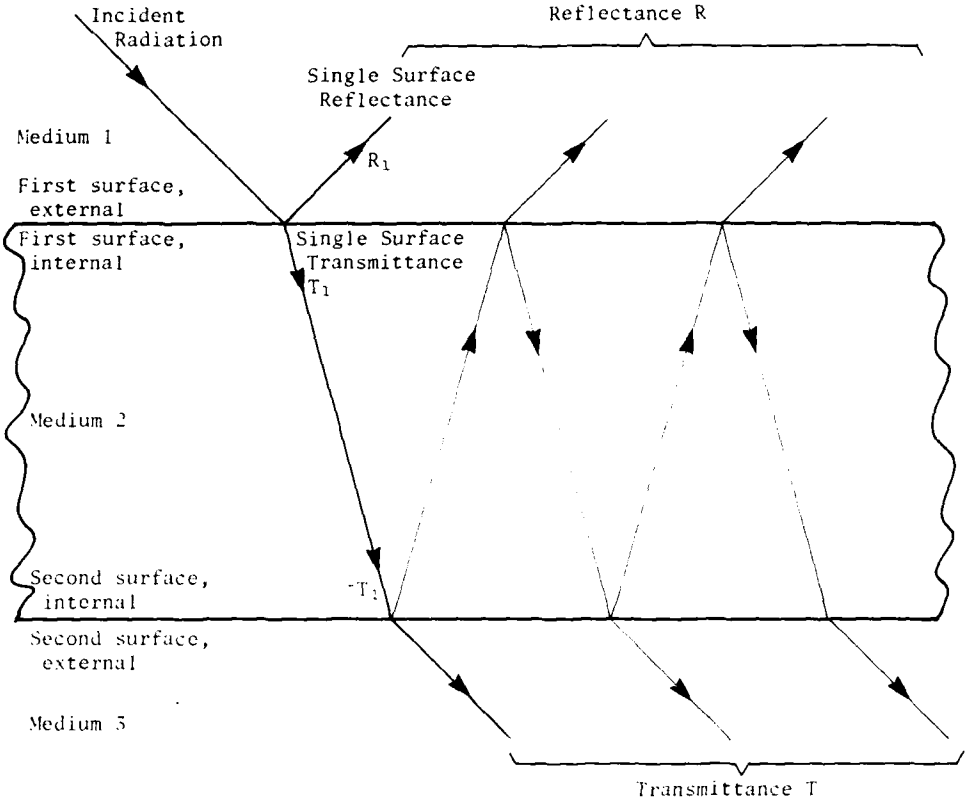

Figure I.1 Schematic ray diagram showing energies of reflected and transmitted components

APPENDIX II

WAVE INTERACTION AT A SIMPLE INTERFACE

Maxwell's equation for the amplitude E of an electromagnetic wave travelling in a medium of permittivity ϵ and magnetic permeability μ with a charge per unit area of σ is given by

$$\nabla^2 E = \mu\sigma \frac{\partial E}{\partial t} + \mu\Sigma \frac{\partial^2 E}{\partial t^2} \qquad \text{(II.1)}$$

One solution, for a wave of initial amplitude E_o and angular frequency w travelling with velocity v in the z direction through an absorbing medium with complex refractive index $\underline{n} = n - ik$ (where n is the real part of the refractive index and k is the absorption index, sometimes known as the extinction coefficient) is given by $E_z = E_o e^{\left[i\left(w\left(t - \frac{z}{v}\right) + \delta\right)\right]}$

$$\text{Amplitude } E_z = E_o e^{\left[i\left(w\left(t - [n - vk]\frac{z}{c}\right) + \delta\right)\right]} \qquad \text{(II.2)}$$

$$= E_o e^{-\frac{wk\,z}{c}} e^{\left[i\left(w\left(t - \frac{nz}{c}\right) + \delta\right)\right]}$$

The complex exponential term represents a wave of frequency w advancing in the z direction with velocity $\frac{c}{n}$ and phase term δ, while the first term represents an attenuation of amplitude as the wave progresses in the z direction. There will be no change in phase while the wave continues within the isotropic medium.

Intensity of the prograting wave is proportional to (Amplitude)^2 ie Intensity is proportional to $e^{-\frac{2wk}{c} z}$.

The conventional expression to describe intensity attenuation in a medium is given by $e^{-\alpha z}$, where the attenuation or absorption coefficient α is defined by considering that over a distance $z = \alpha^{-1}$, the propagating wave intensity is attenuated by a factor e^{-1}.

Using this definition,

$$\alpha = \frac{2wk}{c} = \frac{4\pi k}{\lambda} \qquad \text{(II.3)}$$

When the incident wave given by equation (II.2) reaches a boundary and interacts with a medium having different optical properties to the incident

medium it is split into two waves - a transmitted wave proceeding into the second medium and a reflected wave propagating back into the first (incident) medium.

Applying the boundary conditions at the interface to Maxwell's equation, and using the Maxwell relation

$$\frac{n_2}{n_1} = \frac{v_1}{v_2} = \sqrt{\frac{\Sigma_2 \mu_2}{\Sigma_1 \mu_1}} = \frac{\sin \theta_1}{\sin \theta_2}$$

where the suffixes 1 and 2 refer to the incident medium and the adjacent medium respectively, it is found that the transmitted and reflected waves can be further split into 2 independent amplitude components, respectively parallel (p) and perpendicular (s) to the plance of incidence (see figure II.1).

The Fresnel coefficients r and t for the ratios of reflected/incident and transmitted/incident amplitudes thus each have p and s components

$$\left.\begin{aligned} r_{1p} &= \frac{\underline{n}_2 \cos \underline{\theta}_1 - \underline{n}_1 \cos \underline{\theta}_2}{\underline{n}_2 \cos \underline{\theta}_1 + \underline{n}_1 \cos \underline{\theta}_2} \\ r_{1s} &= \frac{\underline{n}_1 \cos \underline{\theta}_1 - \underline{n}_2 \cos \underline{\theta}_2}{\underline{n}_1 \cos \underline{\theta}_1 - \underline{n}_2 \cos \underline{\theta}_2} \\ t_{1p} &= \frac{2\underline{n}_1 \cos \underline{\theta}_1}{\underline{n}_2 \cos \underline{\theta}_1 + \underline{n}_1 \cos \underline{\theta}_2} \\ t_{1s} &= \frac{2\underline{n}_1 \cos \underline{\theta}_1}{\underline{n}_1 \cos \underline{\theta}_1 + n_2 \cos \underline{\theta}_2} \end{aligned}\right\} \qquad (II.4)$$

For simplicity, now consider normal incidence. We find

$$r_1 = r_{1p} = -r_{1s} = \frac{\underline{n}_2 - \underline{n}_1}{\underline{n}_2 + \underline{n}_1}$$

and

$$t_1 = t_{1p} = t_{1s} = \frac{2\underline{n}_1}{\underline{n}_2 + \underline{n}_1}$$

The sign of r_1 is positive or negative depending on whether $\underline{n}_2$ is greater or less than $\underline{n}_1$. A negative value simply means that the phase of the reflected wave is changed by π relative to that of the incident wave.

When the wave is incident from medium 2 rather than medium 1, the amplitude coefficients become

$$r_2 = r_{2p} = -r_{2s} = \frac{\underline{n}_1 - \underline{n}_2}{\underline{n}_1 - \underline{n}_2} = -r_1$$

and

$$t_2 = t_{2p} = t_{2s} = \frac{2\underline{n}_2}{\underline{n}_1 + \underline{n}_2} = \frac{\underline{n}_2}{\underline{n}_1} \cdot t_1$$

The Fresnel coefficients deal with reflected and transmitted amplitudes while the reflectivity and transmissivity deal with reflected and transmitted energies. Using Poynting's theorem to consider the energy in each medium(ref.II.1) with find that

Transmissivity

$$T_1 = \frac{n_2}{n_1} t_1^2 = \frac{n_1}{n_2} t_2^2 = t_1 t_2$$

Reflectivity

$$R_1 = r_1^2 = r_2^2$$

Since

$$R_1 + T_1 = 1$$

then

$$r_1^2 + t_1 t_2 = 1$$

To investigate possible phase changes upon reflection from and transmission through the interface, consider complex Fresnel coefficients of the form

$$\underline{r}_1 = \sigma_1 e^{i\Delta}$$

where σ_1 and τ_1 are (real) amplitudes and Δ and γ represent phase terms and

$$\underline{t}_1 = \tau_1 e^{i\gamma}$$

1. Reflection

$$r_1 = \frac{\underline{n}_2 - \underline{n}_1}{\underline{n}_2 + \underline{n}_1} = \frac{(n_2 - n_1) - i(k_2 - k_1)}{(n_2 + n_1) - i(k_2 + k_1)}$$

$$= \frac{n_2^2 - n_1^2 + k_2^2 - k_1^2 + 2i\,(n_a k_1 - n_1 k_a)}{(n_2 + n_1)^2 + (k_2 + k_1)^2}$$

$$\tan \Delta = \frac{2(n_1 k_a - n_a k_1)}{n_2^2 - n_1^2 + k_2^2 - k_1^2}$$

If neither medium 1 nor 2 is absorbing, then

$$\tan \Delta = 0$$

so

$$\Delta = 0 \text{ or } \pi$$

ie a phase change of 0 or π takes place upon reflection at an interface when there is no absorption present. If the incident medium is the denser of the two media then the phase change is zero; if the incident medium is less dense then the phase change is π.

If either or both media are absorbing, then $\tan \Delta \neq 0$ and a phase change will take place which is not equal to zero or π.

2. Transmission

$$\underline{t}_1 = \tau_1 e^{i\gamma}$$

$$\underline{t}_1 = \frac{2\underline{n}_1}{\underline{n}_2 + \underline{n}_1} = \frac{(2n_1 - ik_1)}{(n_2 + n_1) - i(k_2 + k_1)}$$

$$= \frac{2(n_1^2 + k_1^2 + n_2n_1 + k_2k_1) + i(n_1k_2 - k_1n_2)}{(n_2 + n_1)^2 + (k_2 + k_1)^2}$$

$$\tan\gamma = \frac{2(n_2k_1 - n_1k_2)}{n_1^2 + k_1^2 + n_1n_2 + k_1k_2}$$

If neither medium 1 nor 2 is absorbing, then

$$\tan\gamma = 0$$

so

$$\gamma = 0 \text{ or } \pi$$

In this situation

$$t_1 = \frac{2n_2}{n_2 + n_1}$$

- always positive so

$$\gamma = 0$$

ie there is never any phase change on transmission through an interface between 2 optically dissimilar non-abosorbing materials.

If either medium is absorbing then there will be a phase change on transmission through the interface. The magnitude of the phase change will depend on all of n_1, n_2, k_1, k_2.

REFERENCES

No.	Author	Title
II.1	Heavens, O.S.	"Optical Properties of Thin Solid Films". London, Butterworths, page 52, 1955

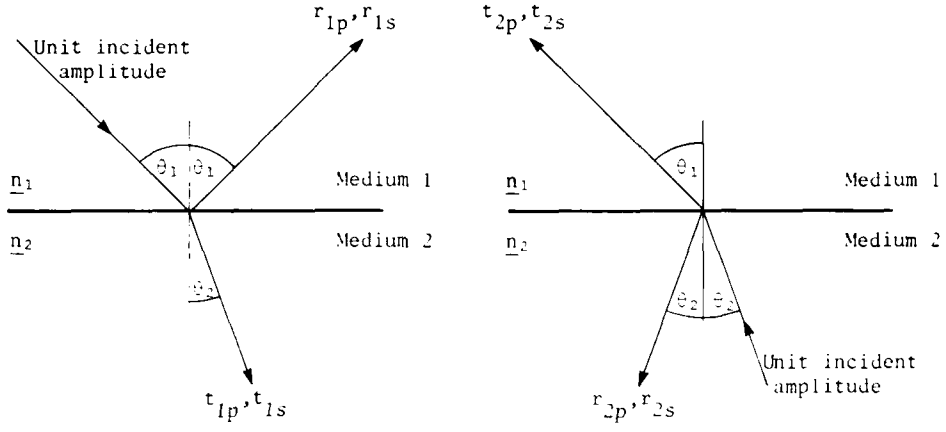

Figure II.1 Fresnel amplitude coefficients for reflection from and transmission through an interface between two media having different optical properties

APPENDIX III

WAVE INTERACTION WITH A FINITE SAMPLE

Consider a plane parallel slab of material of physical thickness d, bounded on both sides by air. The optical properties of the material can be described by real indices n and k defined as refractive index and absorption index respectively.

An incident beam is partially reflected and partially transmitted at each interface, resulting in multiple interference effects. When there is absorption within the material then the beam being reflected back and forth between the two surfaces will be attenuated by the "internal transmittance factors" of the material concerned.

If i_o is the amplitude and $I_o = i_o^2$ is the intensity of the incident wave

r is the Fresnel reflection coefficient from each interface when the wave is incident from the air side of the interface

r_1 is the Fresnel reflection coefficient from each interface when the wave is incident from the material side of the interface

t is the Fresnel transmission coefficient through each interface when the wave is incident from the air side of the interface

t_1 is the Fresnel transmission coefficient through each interface when the wave is incident from the material side of the interface

β is the "internal amplitude transmittance" of the medium between the two interfaces

then the various component beams will have the amplitudes shown in figure III.1.

If ϕ is the total phase change taking place for a single traversal of the sample (ϕ includes contributions associated with internal reflections within the sample, as well as the phase thickness $\frac{2\pi}{\lambda}$ nd cos θ) then, the total phase difference between any two successive transmitted rays (or any two successive reflected rays) is 2ϕ.

When this is taken into account as a factor $e^{-i2\phi}$, and the amplitudes of the various transmitted rays are summed, we obtain

$$\text{Amplitude of the transmitted beam} = i_o \beta t t_1 (1 + \beta^2 r_1^2 e^{-2i\phi} + \beta^4 r_1^4 e^{-4i\phi} + \ldots) \qquad \text{(III.1)}$$

$$= \frac{i_o \beta t t_1}{1 - \beta^2 r_1^2 e^{-2i\phi}}$$

$$\text{Intensity of the transmitted beam} \quad I_T = I_o \left| \frac{\beta t t_1}{1 - \beta^2 r_1^2 e^{-2i\phi}} \right|^2 \qquad \text{(III.2)}$$

where $I_o = i_o^2$ is the intensity of the incident beam.

The internal intensity transmittance β^2 for the material of thickness d is equivalent to an intensity attenuation factor $e^{-\alpha d}$, where α corresponds to the conventional absorption coefficient defined in Appendix II.

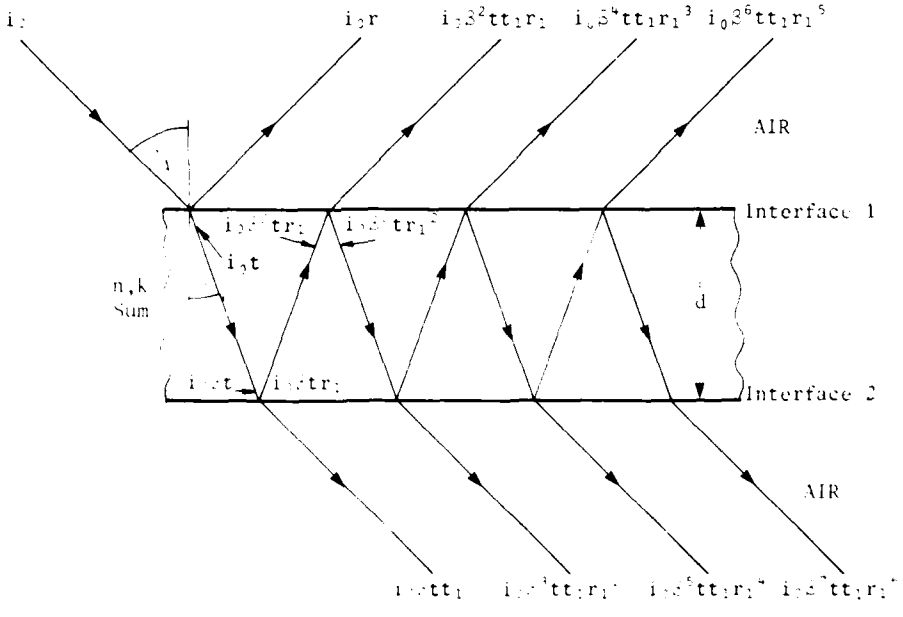

Figure III.1 Multiple beam reflection and transmission in terms of reflection coefficients and transmission coefficients

APPENDIX IV

DERIVATION OF THE EQUATIONS FOR A FABRY-PEROT ETALON

Using the concepts of "equivalent surface" and "equivalent layer" referred to in Appendix I, it is mathematically possible to replace a system of multilayer dielectric stacks, or a finite metallic film, with an equivalent layer or surface, having effective finite reflectivity R_1, transmissivity T_1, absorptivity A_1 and phase properties.

When this is done for the 2 mirrors bounding the spacer layer of a Fabry-Perot filter, and an analysis carried out analogous to that done for a finite sample as in Appendix III, the expressions derived for reflectance and transmittance of the filter are identical with equations (4) and (8) of Appendix III.

ie

$$R = \frac{R_1 \left(1 - (R_1 + T_1)e^{-\alpha d}\right)^2 + 4e^{-\alpha d}(R_1 + T_1)\sin^2\phi}{\left(1 - R_1 e^{-\alpha d}\right)^2 + 4R_1 e^{-\alpha d}\sin^2\phi}$$

$$T = \frac{T_1^2\, e^{-\alpha d}}{\left(1 - R_1 e^{-\alpha d}\right)^2 + 4R_1 e^{-\alpha d}\sin^2\phi}$$

where R_1, T_1, A_1 are properties of each mirror surface and α is the absorption coefficient of the spacer layer of physical thickness d.

The term ϕ defines the total phase change produced by one traversal of the spacer layer.

Since $R_1 + T_1 + A_1 = 1$, we can write the above equations in the form

$$R = \frac{R_1 \left(1 - (1 - A_1)e^{-\alpha d}\right)^2 + 4(1 - A_1)e^{-\alpha d}\sin^2\phi}{\left(1 - R_1 e^{-\alpha d}\right)^2 \left[1 + \dfrac{4R_1 e^{-\alpha d}\sin^2\phi}{\left(1 - R_1 e^{-\alpha d}\right)^2}\right]} \qquad \text{(IV.1)}$$

$$T = \frac{(1 - R_1 - A_1)^2\, e^{-\alpha d}}{\left(1 - R_1 e^{-\alpha d}\right)^2 \left[1 + \dfrac{4R_1 e^{-\alpha d}\sin^2\phi}{\left(1 - R_1 e^{-\alpha d}\right)^2}\right]} \qquad \text{(IV.2)}$$

For the special case when there is no absorption in the spacer layer ($\alpha = 0$) then equation (IV.2) reduces to

$$T = \frac{(1 - R_1 - A_1)^2}{(1 - R_1)^2\,[1 + F\sin^2\phi]}$$

where $F = \frac{4R_1}{(1 - R_1)^2}$ is known as the "Coefficient of Finesse" and the term $\frac{1}{1 + F\sin^2\phi}$ is denoted as the "Airy Function".

THIS IS A BLANK PAGE

DISTRIBUTION

	Copy No.
DEPARTMENT OF DEFENCE	
Defence Science and Technology Organisation	
Chief Defence Scientist	1
Deputy Chief Defence Scientist	
Controller, External Relations, Projects and Analytical Studies	
Superintendent, Science Programs and Administration	
Superintendent, Analytical Studies	2
Electronics Research Laboratory	
Director, Electronics Research Laboratory	3
Mr F.A. Dixon, Electronics Research Laboratory	4
Superintendent, Optoelectronics Division	5
Principal Officer, Night Vision Group	6
Principal Officer, Optical Techniques Group	7
Mr G.W. McQuistan, Optical Techniques Group	8
Mr R.J. Whatmough, Optical Techniques Group	9
Mr J.R. Venning, Optical Techniques Group	10
Mr R.J. Herbert, Optical Techniques Group	11
Mr S.M. Rees, Optical Techniques Group	12
Mr L. Corena, Optical Techniques Group	13
Mr D.E. Verringer, Optical Techniques Group	14
Principal Officer, Surveillance Systems Group	15
Mr P. Wilsen, Surveillance Systems Group	16
Mr M.F. Penny, Surveillance Systems Group	17
Principal Officer, Terminal Guidance Group	18
Principal Officer, Infrared and Optical Countermeasures Group	19
Principal Officer, Systems Integration Group	20
Mr M.R. Meharry, Sensing and Propagation Group	21
Dr D.R. Cutten, Sensing and Propagation Group	22

Mr K.C. Liddiard, Sensing and Propagation Group 23

Mr G.V. Poropat, Sensing and Propagation Group 24

Mr G. Findlay, Sensing and Propagation Group 25

Dr R.H. Hartley, Optoelectronic Device Physics Group 26

Mr P.D. Girdler, Optoelectronic Device, Physics Group 27

Dr J. Richards, Optoelectronic Device, Physics Group 28

Mr B. Furby, Systems Integration Group 29

Mr D.A.B. Fogg, Electronic Warfare Division 30

Weapons Systems Research Laboratory

Director, RAN Research Laboratory 31

Navy Office

Director of Tactics, Action Information Organisation and Navigation 32

Navy Scientific Adviser Cnt Sht Only

Army Office

Director, Operational Requirements 33

Scientific Adviser - Army 34

Director General, Army Development (NSO), Russell Offices for ABCA Standardisation Officers

UK ABCA representative, Canberra 35

US ABCA representative, Canberra 36

Canada ABCA representative, Canberra 37

NZ ABCA representative, Canberra 38

Air Office

Air Force Scientific Adviser 39

Director, Research Requirements 40

Director, Joint Intelligence Organisation (DSTI) 41

Libraries and Information Services

Librarian, Technical Reports Centre, Defence Central Library, Campbell Park 42

Document Exchange Centre
Defence Information Services Branch for:

Microfiche copying 43

ERL-0300-TR

NORTHERN IRELAND

DOCUMENT CONTROL DATA SHEET

Security classification of this page: UNCLASSIFIED

1 DOCUMENT NUMBERS		2 SECURITY CLASSIFICATION	
AR Number:	AR-003-745	a. Complete Document:	Unclassified
Series Number:	ERL-0300-TR	b. Title in Isolation:	Unclassified
Other Numbers:		c. Summary in Isolation:	Unclassified

3 TITLE

FABRY-PEROT TYPE OPTICAL INTERFERENCE FILTERS

4 PERSONAL AUTHOR(S):

M.A. Folkard and
J. Ward

5 DOCUMENT DATE:

August 1986

6 6.1 TOTAL NUMBER OF PAGES

6.2 NUMBER OF REFERENCES 15

7 7.1 CORPORATE AUTHOR(S)

Electronics Research Laboratory

7.2 DOCUMENT SERIES AND NUMBER

Electronics Research Laboratory
0300-TR

8 REFERENCE NUMBERS

a. Task: DST81/112

b. Sponsoring Agency:

9 COST CODE

407742/112

10 IMPRINT (Publishing organisation)

Defence Research Centre Salisbury

11 COMPUTER PROGRAM(S) (Title(s) and language(s))

12 RELEASE LIMITATIONS (of the document)

Approved for public release.

Security classification of this page: UNCLASSIFIED

Security classification of this page: UNCLASSIFIED

13 ANNOUNCEMENT LIMITATIONS (of the information on these pages):

No limitation

14 DESCRIPTORS:

a. EJC Thesaurus Terms

b. Non-Thesaurus Terms

15 COSATI CODES:

16 SUMMARY OR ABSTRACT:
(if this is security classified, the announcement of this report will be similarly classified)

The formulae and theory describing the optical properties of a classical Fabry-Perot interferometer are stated in terms of the reflection, transmission, absorption and phase angle. The appropriate boundary conditions and experimental limitations are defined.

The theory is extended to the production of vacuum deposited, all dielectric, multilayer thin film systems for use as Fabry-Perot type, narrow spectral band filters.

Security classification of this page UNCLASSIFIED

The official documents produced by the Laboratories of the Defence Research Centre Salisbury are issued in one of five categories: Reports, Technical Reports, Technical Memoranda, Manuals and Specifications. The purpose of the latter two categories is self-evident, with the other three categories being used for the following purposes:

Reports	documents prepared for managerial purposes.
Technical Reports	records of scientific and technical work of a permanent value, intended for other scientists and technologists working in the field.
Technical Memoranda	intended primarily for dissemination of information within DSTO. They are usually tentative in nature and reflect the personal views of the author.

END

DATE
FILMED
5-87

DTIC